Naval Research Laboratory

Washington, DC 20375-5320

NRL/MR/5660--04-8819

Monte Carlo Radiative Transfer Simulations for Ocean Optics: A Practical Guide

ROBERT A. LEATHERS
TRIJNTJE VALERIE DOWNES

Applied Optics Branch
Optical Sciences Division

CURTISS O. DAVIS

Remote Sensing Division

CURTIS D. MOBLEY

Sequoia Scientific, Inc.
Bellevue, WA 98005

September 1, 2004

REPORT DOCUMENTATION PAGE

Form Approved
OMB No. 0704-0188

1. REPORT DATE *(DD-MM-YYYY)*	2. REPORT TYPE	3. DATES COVERED *(From - To)*
01-09-2004	Memorandum report	

4. TITLE AND SUBTITLE

Monte Carlo Radiative Transfer Simulations for Ocean Optics: A Practical Guide

5a. CONTRACT NUMBER

5b. GRANT NUMBER

5c. PROGRAM ELEMENT NUMBER
62114N

6. AUTHOR(S)

Robert A. Leathers, Trijntje Valerie Downes, Curtiss O. Davis, and Curtis D. Mobley*

5d. PROJECT NUMBER

5e. TASK NUMBER

5f. WORK UNIT NUMBER
6215-04

7. PERFORMING ORGANIZATION NAME(S) AND ADDRESS(ES)

Naval Research Laboratory
4555 Overlook Avenue, SW
Washington, DC 20375-5320

8. PERFORMING ORGANIZATION REPORT NUMBER

NRL/MR/5660--04-8819

9. SPONSORING / MONITORING AGENCY NAME(S) AND ADDRESS(ES)

Office of Naval Research
800 North Quincy Street
Arlington, VA 22217

10. SPONSOR / MONITOR'S ACRONYM(S)
ONR

11. SPONSOR / MONITOR'S REPORT NUMBER(S)

12. DISTRIBUTION / AVAILABILITY STATEMENT

Approved for public release; distribution is unlimited.

13. SUPPLEMENTARY NOTES

*Sequoia Scientific, Inc., 2700 Richards Road, Suite 107, Bellevue, WA 98005

14. ABSTRACT

This report provides a methodology and the equations needed to generate Monte Carlo computer simulations for many common ocean optics applications. These applications include the modeling of natural ocean-atmosphere environments and analyses of laboratory and in-situ optical instrumentation. We attempt to provide enough practical detail to make it straightforward for the reader to write his/her own computer code for his/her own application. This document also serves as documentation of the methods the authors have used in several specific research projects.

15. SUBJECT TERMS

Monte Carlo; Optical Oceanography

16. SECURITY CLASSIFICATION OF:			17. LIMITATION OF ABSTRACT	18. NUMBER OF PAGES	19a. NAME OF RESPONSIBLE PERSON
a. REPORT	b. ABSTRACT	c. THIS PAGE			Robert A. Leathers
Unclassified	Unclassified	Unclassified	UL	54	19b. TELEPHONE NUMBER *(include area code)* (202) 767-6504

Standard Form 298 (Rev. 8-98)
Prescribed by ANSI Std. Z39.18

CONTENTS

MONTE CARLO RADIATIVE TRANSFER SIMULATIONS FOR OCEAN OPTICS: A PRACTICAL GUIDE

1. INTRODUCTION

This report provides a methodology and the equations needed to generate Monte Carlo computer simulations for many common ocean optics applications. These applications include the modeling of natural ocean-atmosphere environments and analyses of laboratory and in-situ optical instrumentation. We attempt to provide enough practical detail to make it straightforward for the reader to write his/her own computer code for his/her own application. This document also serves as documentation of the methods the authors have used in several specific research projects (e.g., [1]—[3]).

Monte Carlo simulations in this context involve the tracing of the fates of millions of virtual photons or photon packets according to statistical probabilities. The source of the photons being simulated can be either the sun or an artificial light. Each simulated photon path is randomly distinct from the others as determined by the probabilities of absorption and scattering in the water and air and by the probabilities of transmission, reflection, or absorption at air-liquid and liquid-solid interfaces. Example ray-tracing diagrams of Monte Carlo simulations are shown in Figure 1 for the open ocean water column and for a point-source integrating cavity absorption meter (PSICAM). In the ocean case, photons enter at the sea surface, scatter within the water, reflect internally at the sea surface or seafloor, and eventually either escape into the atmosphere or are absorbed by the water or seafloor. In the PSICAM case, photons are initiated at the center of the cavity, internally scattered by the water, internally reflected by the cavity wall, and eventually absorbed by the water or cavity wall. The light intensity at any region in these modeled systems is determined by counting the number of photon paths that intersect that region.

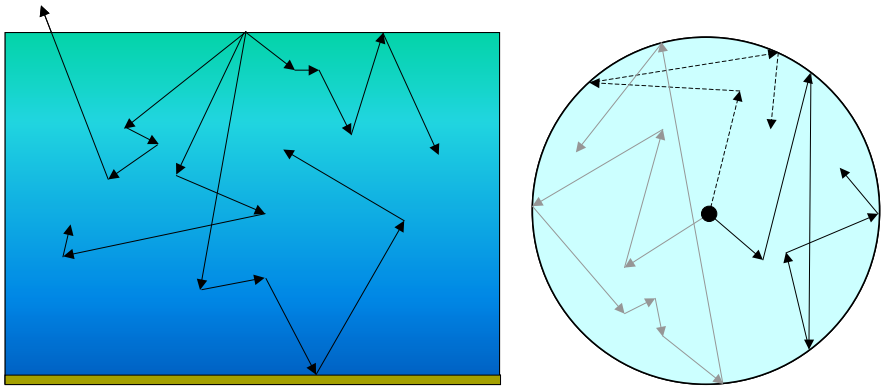

Figure 1 – Forward Monte Carlo simulations of an ocean water column (left) and of an integrating-cavity absorption meter (right).

Manuscript approved July 8, 2004.

The Monte Carlo approach provides the most general and most flexible technique for numerically solving the equations of radiative transfer. Because Monte Carlo techniques are computationally expensive, they have historically been avoided whenever alternative solution techniques are available. However, as computer speeds continue to dramatically improve, the Monte Carlo approach is becoming more practical and popular for all types of radiative transfer calculations. Furthermore, it is no longer imperative that Monte Carlo codes be complicated with tricks designed to save computer memory and to avoid expensive commands (i.e., logical statements and trigonometric functions). This makes Monte Carlo techniques accessible now to anyone with basic programming skills.

Monte Carlo techniques have been used by various researchers in the ocean optics community over the last several decades [1]—[20], and introductions to the use of Monte Carlo techniques in ocean optics are provided in Refs. 21 and 22. References on the use of Monte Carlo methods for the study of light propagation in the atmosphere [23] and in biological tissue [24, 25] are also relevant. Most of the cited references discuss very specific applications and fail to provide sufficient detail to reproduce their Monte Carlo simulations; however, they at least provide insight into general Monte Carlo methodology. In this report we compile much of the practical information provided in the references and add lessons learned from our own research. We introduce some basic ocean optics and Monte Carlo concepts in Section 2, describe how to move a photon from one interaction point to another in Section 3, and show how to compute scattering angles in Sections 4. A description of how to simulate photon sources and detectors is provided in Sections 5 and 6. The interactions of photons with surfaces, such as the sea surface and seafloor are discussed in Section 7. Backward Monte Carlo techniques are introduced in Section 8. A short summary of the most frequently used Monte Carlo equations is provided in Section 9. In Section 10 we provide many examples of Monte Carlo codes relevant to Ocean Optics and evaluate their performance.

2. PRELIMINARIES

2.1 Nomenclature

The terminology in this report is a combination of that from radiative transfer theory (as applied in optical oceanography) and that from probability and statistics. For the former, we adopt the nomenclature from Mobley [21]. For example, the processes of absorption and scattering by seawater are quantified by the beam absorption coefficient a (m^{-1}), the scattering coefficient b (m^{-1}), and the scattering phase function $\tilde{\beta}$. The beam attenuation coefficient c (m^{-1}) and single scattering albedo ω_0 are related to a and b by $c = a+b$ and $\omega_0 = b/c$. These symbol definitions, as well as others used in this report, are provided in Table 1.

Table 1 - Nomenclature

A	beam absorption coefficient (m^{-1})
B	beam scattering coefficient (m^{-1})
b_r, $b_{r;q}$	Raman scattering coefficient
C	beam attenuation coefficient (m^{-1}), $c = a+b$
E_0	scalar irradiance (W/m^2)
E_d	downward irradiance (W/m^2)
E_u	upward irradiance (W/m^2)

G	scattering phase function asymmetry factor
$\hat{i}, \hat{j}, \hat{k}$	unit vectors along x, y, and z axes
L	optical pathlength
N	index of refraction
$\hat{n}$	outward normal to a surface (unit vector)
P	cumulative distribution function (CDF)
p	probability density function (PDF)
R	irradiance ratio
R_b	seafloor albedo
R_i	internal reflectance at water-air interface
q	random number uniform on [0,1]
s	geometric pathlength (m)
w	photon weight
x, y, z	Cartesian coordinates
$\vec{x}$	position vector, $\vec{x} = [x\hat{i}, y\hat{j}, z\hat{k}]$
z_b	water depth (m)
$\tilde{\beta}$	scattering phase function
θ	polar angle with respect to the z-axis
θ_i	incident polar angle with respect to the normal to a surface
θ_t	transmitted polar angle with respect to the normal to a surface
λ	Wavelength
ν	Frequency
μ_s	cosine of polar angle with respect to photon direction or with respect to the normal to a surface.
μ_x	direction cosine with respect to x-axis
μ_y	direction cosine with respect to y-axis
μ_z	direction cosine with respect to z-axis
ρ	surface reflectivity
τ	optical depth
Φ	azimuthal angle with respect to direction of photon travel
ϕ	azimuthal angle with respect to the x-axis
$\hat{\xi}$	unit-magnitude direction vector
Ψ	polar angle with respect to direction of photon travel
Ω	solid angle
ω_0	single-scattering albedo, $\omega_0 = b/c$

2.2 Probability Functions and Random Numbers

Monte Carlo simulations rely on properly defined probability density functions and cumulative distribution functions. In general the probability density function $p(x)$ is defined such that the probability that a specified event will occur over the range x to $(x+\mathrm{d}x)$ is $[p(x)\,\mathrm{d}x]$ and

$$\int_{-\infty}^{\infty} p(x)dx = 1. \tag{2.1}$$

The cumulative distribution function $P(x)$ is the probability that the specified event will occur between the lowest possible value of x (frequently 0, but more generally $-\infty$) and x,

$$P(x) = \int_{-\infty}^{x} p(x)dx, \qquad 0 \le P(x) \le 1. \tag{2.2}$$

To determine the value of x for a particular Monte Carlo realization, we select a random number q from the uniform distribution over [0,1], set it equal to the cumulative distribution function [21],

$$P(x) = q, \tag{2.3}$$

and solve for x. We solve for x either analytically or numerically, depending on the form of $P(x)$. Many examples of the use of Eq. (2.3) are provided throughout this report. It is important to note that a particular value of q is never used more than once. If consecutive equations contain q, each q represents a distinct random number. This is consistent with the way random number generators are used in computer languages. For example, when writing code for Matlab (The MathWorks, Inc), the variable q can simply be replaced with the keyword *rand*. At each and every occurrence of rand, Matlab will substitute a new random number.

2.3 Photon Weights and Biasing

Because it is computationally wasteful to trace the full paths of photons that never reach a spatial region of interest, it is frequently prudent to sample from a biased cumulative distribution function. Biasing the distribution function makes it possible to trace more photons that are likely to find their way to areas of interest and fewer photons that are unlikely to, without changing the final computed result. This makes it possible to converge more quickly to a result of specified accuracy. If the probability function is $p(x)$, but we prefer to trace photons according to the biased probability density function $p_b(x)$ so that more photons reach regions of interest, we can use $p_b(x)$ as long as we multiply the photon weight by the ratio of the correct distribution to the biased one [21],

$$w = w\left(\frac{p(x)}{p_b(x)}\right). \tag{2.4}$$

An example of biased sampling is given in Sect 3.1; additional examples are provided by Mobley [21].

We use a similar idea to treat the absorption of photons within the water column and at surfaces. Rather than computing the probability of absorption and then terminating the photon path if the photon is absorbed, we trace a photon to an event (scattering or reflecting) and then reduce its weight based by the statistical probability that absorption would have taken place. We then continue to trace the photon path as if it had not been absorbed. An alternative way to think of this is that we initially launch a packet of many photons traveling in the same direction and we reduce the number of photons in the packet at each event by the number of photons that would have been absorbed by the event. Specifically, we multiply the photon weight by the value of the single-scattering albedo ω_0 each time it is scattered and by the value of the surface albedo each time it is reflected by a surface. Only when the weight of a photon is reduced to below a certain specified level do we stop tracing the photon path.

3. PHOTON TRAVEL

3.1 Path Length

From the definition of optical distance l, the probability density function for the attenuation of light with respect to optical distance traveled is [21]

$$p(l) = e^{-l}, \quad l \geq 0 . \tag{3.1}$$

From Eq. (2.2), the cumulative distribution function is [21]

$$P(l) = \int_0^l e^{-l'} dl' = 1 - e^{-l} \quad . \tag{3.2}$$

To determine l for Monte Carlo simulations, let $P(l) = q$ [Eq. (2.3)] and solve for l [21],

$$l = -\ln(1-q) = -\ln(q) , \quad 0 \leq q \leq 1 . \tag{3.3}$$

Shown in Figure 2 are plots of $p(l)$, $P(l)$, and $l(q)$ as given by Eqs. (3.1) – (3.3).

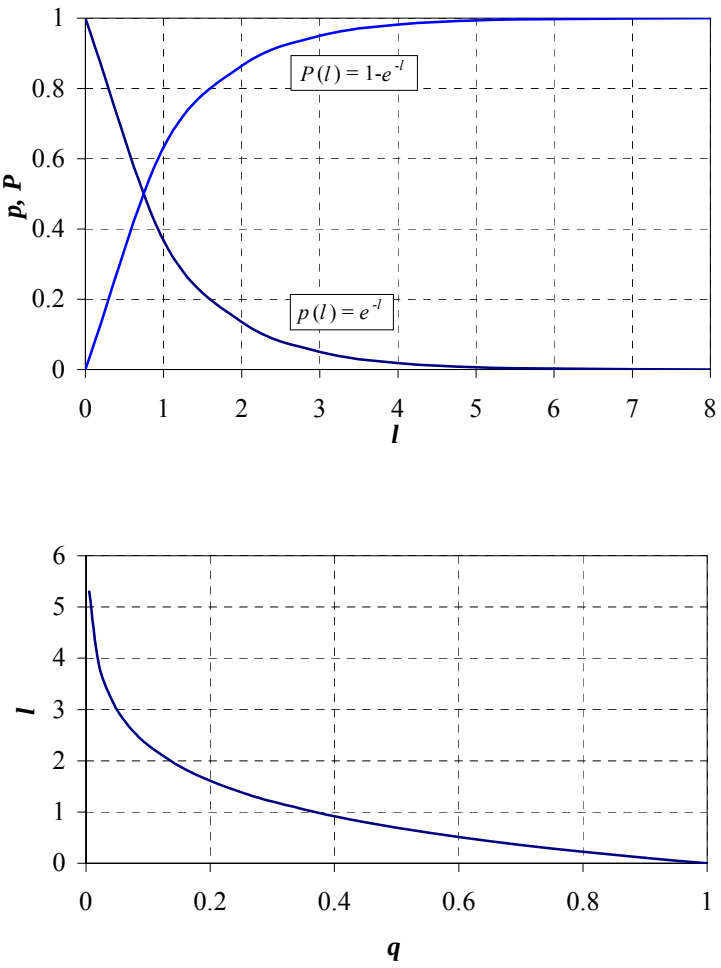

Figure 2 – Probability functions for pathlength determination and pathlength (*l*) versus random number (*q*).

In homogenous waters, the geometric pathlength s (in meters) can be computed with [21, 22]

$$s = \frac{l}{c} = -\frac{\ln(q)}{c}, \tag{3.4}$$

where c is the attenuation coefficient (m^{-1}). In nonhomogenous waters, the relationship between s and l is given by

$$l = \int_0^s c(s')ds', \tag{3.5}$$

and the value of s must be computed by starting at zero and increasing its value until the total value of l computed with Eq. (3.5) equals that given by Eq. (3.3). In a layered system, the integral in Eq. (3.5) becomes a summation.

A simple Monte Carlo code that relies primarily on Eq. (3.4) is provided in Section 10.1.

Equation (3.3) gives the probability density function for the distance an unimpeded photon travels before being scattered or absorbed. However, if there is a highly absorbing boundary present, it is computationally wasteful to track a high number photons that collide with this boundary. We can instead sample from a biased density function that only considers photons that are scattered before reaching the boundary [19],

$$p(l) = \frac{\exp(-l)}{1-\exp(-l_b)}, \quad 0 \le l \le l_b ,$$

where l_b is the optical distance to the boundary along the direction of travel. To compensate for the biased probability function, we multiply the weight of the photon packet by [1 - exp(-l_b)], which is the fraction of the photons that do not reach the boundary. The cumulative distribution function is

$$P(l) = \int_0^l p(l')dl' = \frac{e^{-l+l_b} - e^{-l} - e^{l_b} + 1}{-e^{l_b} + 2 - e^{-l_b}} .$$

Note that $P(l_b) = 1$. Solving $P(l) = q$, we obtain

$$l = l_b - \ln\left[\exp\left(l_b\right) + \left(1 - \exp\left(l_b\right)\right)q\right].$$

3.2 Direction Cosines

The direction cosines μ_x, μ_y, and μ_z are the x, y, and z components of the unit vector that points in the direction of photon travel. By definition, they satisfy

$$\mu_x^2 + \mu_y^2 + \mu_z^2 = 1 .$$

Given the direction cosines and the photon path length s, we can advance the photon from its previous position (x_0,y_0,z_0) to its next location with

$$x = x_0 + \mu_x s ,$$

$$y = y_0 + \mu_y s ,$$

$$z = z_0 + \mu_z s .$$

For a direction defined by polar angle θ ($0 \le \theta \le \pi$) and azimuthal angle ϕ ($0 \le \phi \le 2\pi$),

$$0 \le \theta \le \pi, \quad 0 \le \phi \le 2\pi ,$$

the corresponding direction cosines are

$$\mu_x = \sin\theta\cos\phi , \tag{3.6}$$

$$\mu_y = \sin\theta\sin\phi , \tag{3.7}$$

$$\mu_z = \cos\theta . \tag{3.8}$$

Because $0 \le \theta \le \pi$, $\sin\theta$ is always positive and can be determined from μ_z with

$$\sin\theta = \sqrt{1-\mu_z^2} \ .$$

Frequently we know μ_z and ϕ, from which we can find μ_x and μ_y with

$$\mu_x = \sqrt{1-\mu_z^2}\cos\phi \ ,$$

$$\mu_y = \sqrt{1-\mu_z^2}\sin\phi \ .$$

To compute θ and ϕ from the direction cosines we can use

$$\theta = \cos^{-1}\mu_z \ ,$$

$$\phi = \cos^{-1}\left(\frac{\mu_x}{\sqrt{1-\mu_z^2}}\right), \quad \mu_z^2 \ne 1, \quad \mu_y \ge 0 \ ,$$

$$\phi = 2\pi - \cos^{-1}\left(\frac{\mu_x}{\sqrt{1-\mu_z^2}}\right), \quad \mu_z^2 \ne 1, \quad \mu_y < 0 \ .$$

If $\mu_z^2 = 1$, then $\mu_x = \mu_y = 0$, making ϕ indeterminate. In this case, ϕ can be set randomly.

3.3 Time-Dependent Simulations

If we wish to compute how long it takes for light to find its way from source to detector, we can compute the time it takes each photon to trace its path. The time required for a photon to move a geometric pathlength s is

$$t = s/c_n = s\,n/c_0 \ ,$$

where c_0 is the speed of light in vacuo and c_n is the speed of light in a medium with index of refraction n.

4 SCATTERING

4.1 Scattering Probabilities

4.1.1 Basic equations

The scattering phase function $\tilde{\beta}(\Psi,\Phi)$ is the probability density function that gives the probability that a photon, when scattered, will scatter at polar angle Ψ and azimuthal angle Φ away from the incident direction [21]. From Eq. (2.1), the integral of $\tilde{\beta}(\Psi,\Phi)$ over all directions is unity,

$$\int_0^{2\pi}\int_0^{\pi}\tilde{\beta}(\Psi,\Phi)\sin(\Psi)d\Psi d\Phi = 1\,. \tag{4.1}$$

The $\sin(\Psi)$ term in this equation arises from the definition of the spherical coordinate system. For seawater and for air, the scattered azimuthal angle Φ with respect to the incident direction is uniformly distributed over $[0,2\pi]$. Therefore $p(\Psi)$ and $p(\Phi)$ are independent of one another and

$$p(\Psi,\Phi) = p(\Psi)\,p(\Phi).$$

In order to satisfy Eq. (2.1),

$$\int_0^{2\pi} p(\Phi)d\Phi = 1\,,$$

the probability density function for Φ must be

$$p(\Phi) = \frac{1}{2\pi}\,. \tag{4.2}$$

From Eq. (2.2)

$$P(\Phi) = \int_0^{\Phi}\frac{1}{2\pi}d\Phi = \frac{\Phi}{2\pi}\,,$$

and from Eq. (2.3) [21]

$$\Phi = 2\pi q\,. \tag{4.3}$$

Alternatively, one can use two random numbers q_1 and q_2 to determine Φ with [23]

$$W_1 = 1-2q_1\,,\quad W_2 = 1-2q_2\,,$$

$$d = \sqrt{W_1^2+W_2^2}\,,$$

$$\cos\Phi = W_1/d\,,\ \ \sin\Phi = W_2/d\,. \tag{4.4}$$

Because for seawater and air $\tilde{\beta}(\Psi,\Phi)$ does not depend on Φ, Eq. (4.1) simplifies to

$$2\pi\int_0^{\pi}\tilde{\beta}(\Psi)\sin(\Psi)d\Psi = 1\,. \tag{4.5}$$

From Eqs. (2.1) and (4.5) [21],

$$p(\Psi) = 2\pi\tilde{\beta}(\Psi)\sin(\Psi)\,. \tag{4.6}$$

From Eqs. (2.2), (2.3), and (4.6) [21],

$$P(\Psi) = \int_0^{\Psi} p(\Psi)d\Psi = 2\pi\int_0^{\Psi}\tilde{\beta}(\Psi)\sin(\Psi)d\Psi = q\,. \tag{4.7}$$

Alternatively, if we express the scattering phase function in terms of the cosine of the scattering angle,

$$\mu_s = \cos\Psi, \qquad d\mu_s = -\sin(\Psi)d\Psi$$

then Eqs. (4.5) – (4.7) become

$$-2\pi\int_1^{-1}\tilde{\beta}(\mu_s)d\mu_s = 2\pi\int_{-1}^{1}\tilde{\beta}(\mu_s)d\mu_s = 1\,, \tag{4.8}$$

$$p(\mu_s) = 2\pi\tilde{\beta}(\mu_s)\,, \tag{4.9}$$

$$P(\mu_s) = \int_{\mu_s}^{1} p(\mu)d\mu = 2\pi\int_{\mu_s}^{1}\tilde{\beta}(\mu)d\mu = q\,. \tag{4.10}$$

For a given phase function, one must evaluate the integral in Eq. (4.7) or (4.10) and solve for Ψ or μ_s in terms of q.

We note that some authors define $\tilde{\beta}(\mu_s)$ such that its integral equals unity, as opposed to Eqs. (4.5) and (4.8) that contain a 2π term. If so, then Eqs. (4.9) and (4.10) must also have the 2π term removed; i.e.,

$$\int_{\mu_s}^{1}\tilde{\beta}(\mu)d\mu = q$$

if and only if

$$\int_{-1}^{1}\tilde{\beta}(\mu)d\mu = 1\,.$$

4.1.2 Isotropic scattering

For all specific cases we will consider the azimuthal scattering angle Φ is determined with Eq. (4.3),

$$\Phi = 2\pi q\,.$$

For isotropic scattering $\tilde{\beta}$ is constant by definition. In order to satisfy Eqs. (4.5) and (4.8) ,

$$\tilde{\beta}(\Psi) = \tilde{\beta}(\mu_s) = \frac{1}{4\pi}.$$

From Eqs. (4.6) and (4.9),

$$p(\Psi) = \frac{1}{2}\sin(\Psi),$$

$$p(\mu_s) = \frac{1}{2},$$

and from Eq. (4.10),

$$\frac{1}{2}\int_0^{\Psi_s} \sin(\Psi) d\Psi = \frac{1}{2}(1-\cos\Psi) = q,$$

or

$$\frac{1}{2}\int_{\mu_s}^{1} d\mu = \frac{1}{2}(1-\mu_s) = q.$$

Thus the polar scattering angle is determined with

$$\mu_s = \cos\Psi_s = 1-2q. \tag{4.11}$$

Plots of $\mu_s(q)$ and $\Psi(q)$ for isotropic scattering are shown in Figure 4.

4.1.3 Rayleigh, Raman, and pure water scattering

Rayleigh, Raman, and Pure-water scattering phase function are of the form

$$\tilde{\beta} \propto 1 + f\mu^2,$$

where f is a scalar constant. Specifically, scattering for pure water obeys [21,22]

$$\tilde{\beta} \propto 1 + 0.835\mu^2,$$

and Raman scattering at 490 nm follows [21,22]

$$\tilde{\beta} \propto 1 + 0.55\mu^2.$$

For a given value of f (e.g., 0.835 for pure water) we can normalize the probability density function such that its integral from $\mu = -1$ to 1 is unity,

$$p(\mu) = \frac{3}{2}\frac{1+f\mu^2}{3+f}.$$

Integrating, we obtain the cumulative distribution function,

$$P(\mu) = -\frac{f}{6+2f}\mu^3 - \frac{3}{6+2f}\mu + \frac{1}{2}.$$

To find a value for μ in Monte Carlo simulations, we set $P(\mu) = q$ and solve for q. Therefore, the value of μ is the real root of

$$-\frac{f}{6+2f}\mu^3 - \frac{3}{6+2f}\mu + \frac{1}{2} - q = 0. \tag{4.12}$$

Equation (4.12) can be solved either analytically (which has a complicated form) or numerically. Figure 3 shows the relationship between random number q and polar scattering direction μ_s for pure water as computed by substituting $f = 0.835$ into Eq. (4.12).

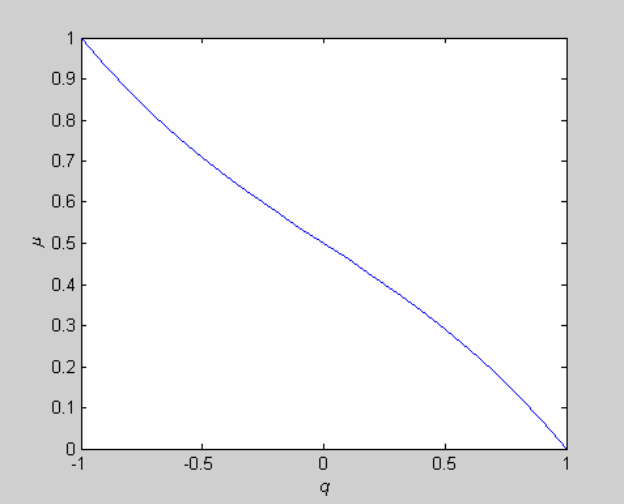

Figure 3 – Determination of the cosine of the scattering angle from random number q for pure water.

4.1.4 Henyey-Greenstein scattering phase function

The Henyey-Greenstein phase function [26] is defined in terms of the asymmetry factor g,

$$\tilde{\beta}(g;\Psi_s) = \frac{1}{4\pi}\frac{1-g^2}{(1+g^2-2g\cos\Psi_s)^{3/2}}, \quad -1 < g < 1,$$

$$\tilde{\beta}(g;\mu_s) = \frac{1}{4\pi}\frac{1-g^2}{(1+g^2-2g\mu_s)^{3/2}}, \quad -1 < g < 1, \tag{4.13}$$

where $g = 0$ reduces to isotropic scattering and g close to 1 describes very forward scattering. Equation (4.13) satisfies Eq. (4.8), and from Eq. (4.9),

$$p(\Psi_s) = \frac{1}{2}\frac{(1-g^2)\sin\Psi_s}{(1+g^2-2g\cos\Psi_s)^{3/2}},$$

$$p(\mu_s) = \frac{1}{2}\frac{1-g^2}{(1+g^2-2g\mu_s)^{3/2}}\,.$$

From Eq. (4.10),

$$P(\mu_s) = \frac{1-g^2}{2}\int_{\mu_s}^{1}\frac{1}{(1+g^2-2g\mu_s)^{3/2}}\,,$$

$$= \frac{1-g^2}{2g}\left(\frac{1}{1-g} - \frac{1}{\sqrt{1+g^2-2g\mu_s}}\right) = q\,.$$

Solving for μ_s ,

$$\mu_s = \frac{2g+1-2qg-2q+2q^2g+g^2-2g^3q-2qg^2+2g^3q^2}{\left(-g-1+2qg\right)^2}\,.$$

For convenience, this can be rewritten as

$$\mu_s = \frac{1}{2g}\left[1+g^2-\left(\frac{1-g^2}{1+g-2gR}\right)^2\right], \quad g \neq 0,$$

$$\mu_s = 1-2g, \qquad g = 0.$$

Note that if we substitute (1-q) for q, we obtain an alternative form [24,25],

$$\mu_s = \frac{1}{2g}\left[1+g^2-\left(\frac{1-g^2}{1-g+2gR}\right)^2\right], \quad g \neq 0\,.$$

The value of μ_s is plotted versus random number q for several different values of g in Figure 4. For $g = 0$, the scattering is isotropic (Sect.4.1.2).

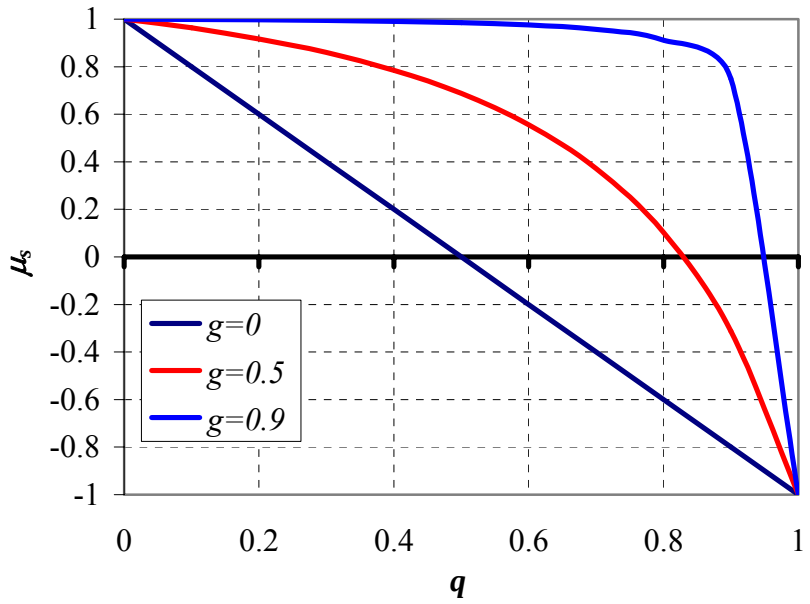

Figure 4 – Polar scattering angle versus random number q for isotropic scattering ($g = 0$) and Henyey-Greenstein scattering with anisotropy factors of $g = 0.5$ and 0.9

4.1.5 Measured scattering phase functions

Few measurements of the scattering phase function have been made in natural waters. The most well known are those made by Petzold [27]; other early measurements are summarized by Jerlov [28]. One way to use such measurements in Monte Carlo codes is to tabulate the cumulative distribution function as a function of q and use interpolation to compute Ψ for each q.

Kirk [4] computed the cumulative distribution function for the Petzold measurement made in San Diego Harbor. This is included here in Table 2 and Figure 5. Similarly, the Petzold average particle phase function [11] can be integrated to obtain its CDF.

Table 2- Cumulative distribution function versus scattering angles for Petzold's San Diego scattering phase function (computed from Kirk [9]).

$P(\theta_s)$	θ_s	μ_s	$P(\theta_s)$	θ_s	μ_s
0.517	2.5	0.999048	0.9832	92.5	-0.04362
0.666	7.5	0.991445	0.9853	97.5	-0.13053
0.751	12.5	0.976296	0.987	102.5	-0.21644
0.811	17.5	0.953717	0.9888	107.5	-0.30071
0.851	22.5	0.92388	0.9902	112.5	-0.38268
0.879	27.5	0.887011	0.9917	117.5	-0.46175
0.901	32.5	0.843391	0.9928	122.5	-0.5373
0.918	37.5	0.793353	0.9941	127.5	-0.60876
0.931	42.5	0.737277	0.995	132.5	-0.67559
0.942	47.5	0.67559	0.996	137.5	-0.73728
0.95	52.5	0.608761	0.9968	142.5	-0.79335

0.957	57.5	0.5373	0.9976	147.5	-0.84339
0.963	62.5	0.461749	0.9982	152.5	-0.88701
0.968	67.5	0.382683	0.9988	157.5	-0.92388
0.972	72.5	0.300706	0.9992	162.5	-0.95372
0.975	77.5	0.21644	0.9997	167.5	-0.9763
0.978	82.5	0.130526	0.9998	172.5	-0.99144
0.981	87.5	0.043619	1.0000	177.5	-0.99905

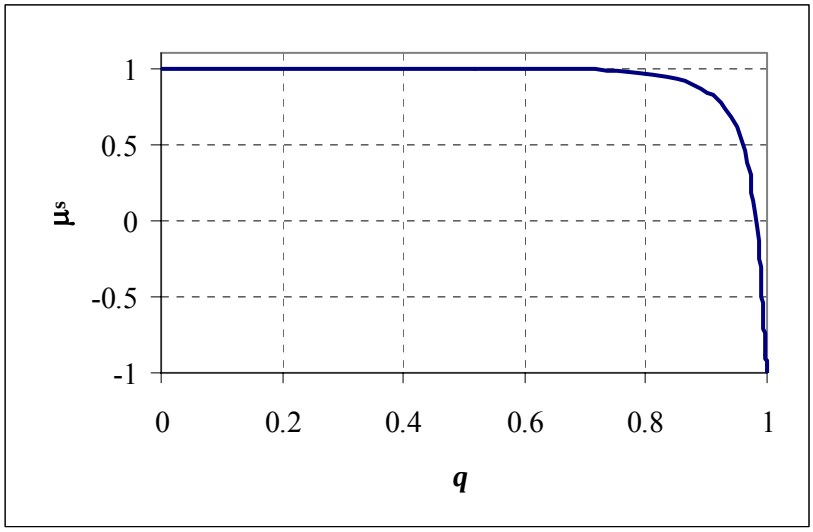

Figure 5 – Cosine of polar scattering angle versus random number q for Petzold's San Diego Harbor scattering phase function.

To avoid having to interpolate tables, Haltrin [8] suggested using an empirical fits to these functions. He provides mathematical expressions for many different measured scattering phase functions, including those obtained by Petzold, Kopelevich, Man'kovsky, and others.

4.2 Updating The Direction Cosines

Given an initial direction defined by θ and ϕ and the scattering angles Ψ and Φ with respect to the initial direction, we need to determine the new direction cosines, μ_x', μ_y', and μ_z'. If we let **a** represent the unit vector in the direction of the initial photon direction,

$$\mathbf{a} = [\mu_x, \mu_x, \mu_x],$$

then the new direction unit vector is given by

$$\hat{\mathbf{a}} = \sin\Psi\cos\Phi\mathbf{a}_\perp \times \mathbf{a} + \sin\Psi\sin\Phi\mathbf{a}_\perp + \cos\Psi\mathbf{a},$$

where $\mathbf{a}_\perp$ is a unit vector perpendicular to $\hat{\mathbf{a}}$. Because $\mathbf{a}_\perp$ is not unique, there is not a unique formula for updating the direction cosines. If we choose $\mathbf{a}_\perp$ to lie in the x-y plane, then

$$\mathbf{a}_\perp = \pm\left[-\mu_y, \mu_x, 0\right]/\sqrt{1-\mu_z^2},$$

$$\mathbf{a}_{\perp} \times \hat{\mathbf{a}} = \pm\left[\mu_x\mu_z, \mu_y\mu_z, -\left(1-\mu_z^2\right)\right] / \sqrt{1-\mu_z^2} \ .$$

If the photon is very close to the z-axis (e.g., $|\mu_z| > 0.99999$) then it is preferable to update the direction cosines with [25]

$$\mu_x' = \sin\Psi\cos\Phi \ ,$$

$$\mu_y' = \sin\Psi\sin\Phi,$$

$$\mu_z' = \frac{\mu_z}{|\mu_z|}\cos\Psi = \text{sign}(\mu_z)\cos\Psi.$$

Putting this all together, the new direction cosines can be determined from the initial photon direction, the cosine of the polar scattering angle μ_s ($\mu_s = \cos\Psi$), and the azimuthal scattering angle Φ with [1, 23, 25],

$$\begin{bmatrix} \mu_x' \\ \mu_y' \\ \mu_z' \end{bmatrix} = \begin{bmatrix} \mu_x\mu_z \Big/ \sqrt{1-\mu_z^2} & -\mu_y \Big/ \sqrt{1-\mu_z^2} & \mu_x \\ \mu_y\mu_z \Big/ \sqrt{1-\mu_z^2} & \mu_x \Big/ \sqrt{1-\mu_z^2} & \mu_y \\ -\sqrt{1-\mu_z^2} & 0 & \mu_z \end{bmatrix} \begin{bmatrix} \sqrt{1-\mu_s^2}\cos\Phi \\ \sqrt{1-\mu_s^2}\sin\Phi \\ \mu_s \end{bmatrix}, \quad \mu_z^2 < 1 \qquad (4.14)$$

$$\begin{bmatrix} \mu_x' \\ \mu_y' \\ \mu_z' \end{bmatrix} = sign\left(\mu_z\right) \begin{bmatrix} \sqrt{1-\mu_s^2}\cos\Phi \\ \sqrt{1-\mu_s^2}\sin\Phi \\ \mu_s \end{bmatrix}, \quad \mu_z^2 \approx 1.$$

In plane parallel problems where μ_z is the only direction cosine that we need to keep track of, we can update μ_z simply with [4]

$$\mu_z' = \mu_z\,\mu_s \mp \sqrt{1-\mu_z^2}\sqrt{1-\mu_s^2}\cos\Phi \ .$$

As a consistency check, any transformation should satisfy

$$\mu_s = [\mu_x, \mu_y, \mu_z] \cdot [\mu_x', \mu_y', \mu_z']$$

and

$$\sqrt{(\mu_x')^2 + (\mu_y')^2 + (\mu_z')^2} = 1 \ .$$

4.3 Inelastic Scattering

In inelastic scattering, some of the light at a given wavelength is removed and reemitted at a longer wavelength. Specifically, we are concerned with the Raman scattering of liquid water. The difference in the frequencies of the incident and scattered light is defined as the Raman shift ν_r [21, 29, 30],

$$\nu_r = \nu_s - \nu' .$$

The amount of Raman scattering present can be quantified by the Raman scattering coefficient $b_{r;q}$ (m^{-1}), which is the ratio of scattered quanta per second at ν_s to the incident quanta per second at ν'. This coefficient is an inherent optical property and [30]

$$a + b + b_{r;q} = c ,$$

although usually the Raman coefficient is implicitly included in the value of a [21].

The quantity $b_{r;q}$ is related to b_r, which is the ratio of scattered power at ν_s to the incident power at ν', by [30]

$$b_{r;q} = \left(\frac{\nu'}{\nu_s} \right) b_r .$$

The wavelength dependence of b_r is given by [21]

$$b_r(\lambda') = \left(\frac{\lambda_0'}{\lambda'} \right)^4 b_r(\lambda_0'),$$

where λ_0 is a reference wavelength; b_r can be taken to be 2.4 x 10^{-4} m^{-1} for $\lambda_0' = 488$ nm.

One way to handle inelastic scattering in Monte Carlo codes is to simulate detectors counting photons at multiple wavelengths (the excitation wavelength and several other longer wavelengths). Following Waters [29], we used a random number to determine whether or not a photon had undergone an inelastic scatter (based on the probability quantified by b_r). If so, another random number was used to determine the frequency shift. If the new wavelength for the photon was within one of the wavelength bands being measured, then we continue to trace the photon at the new wavelength.

The Raman scattering direction can be determined by substituting $f = 0.55$ into Eq. (4.12),

$$-0.1549\mu_s^3 - 0.4225\mu_s + 0.5 = q .$$

One must either solve for μ_s for each random number q or tabulate μ versus q and then read μ from the table. Example values are provided in Table 3.

Table 3 – Cosine of Raman scattering direction versus random number q.

q	μ_s
0.0000	-1.0000
0.1111	-0.8195
0.2222	-0.6148
0.3333	-0.3841
0.4444	-0.1311
0.5556	0.1311

0.6667	0.3841
0.7778	0.6148
0.8889	0.8195
1.0000	1.0000

The shift in wavenumber can be approximated with [29]: a zero probability for shifts less than 2975 cm^{-1}, a linear increase from 2975 to 3175 cm^{-1}, a uniform distribution from 3175 to 3425 cm^{-1}, a linear decrease from 3425 to 3725 cm^{-1}, and a zero probability above 3725 cm^{-1}. Normalizing this piecewise-linear probability density function (PDF), we obtain the four-point function shown in Table 4. A more complex model for the Raman scattering PDF is provided by Mobley [21].

Table 4 – Probability density function for Raman shift in wavenumber [20].

wavenumber κ (cm^{-1})	$p(\kappa)$
2975	0
3175	0.002
3425	0.002
3725	0

The cumulative distribution function (CDF) is obtained by integrating the probability density function. For practical use it can either be tabulated or approximated by an analytic function. The CDF for the PDF of Table 4 is plotted in Figure 6 and tabulated in Table 5.

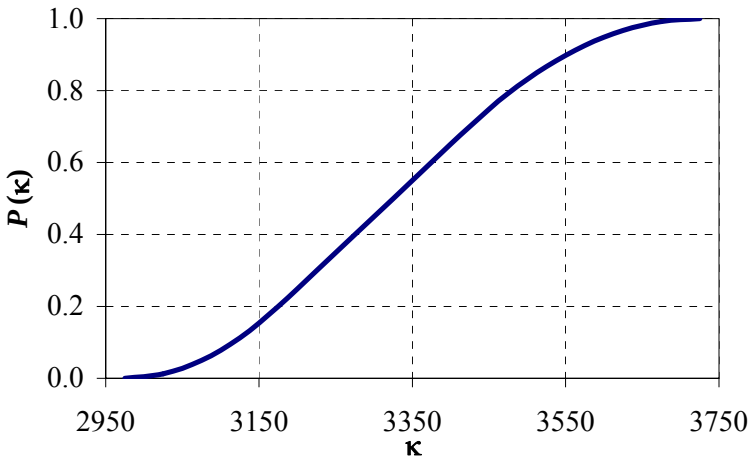

Figure 6 – Cumulative distribution function for the Raman wavenumber shift as computed from Table 3.

Table 5 – Cumulative distribution function for Raman wavenumber shift (from Figure 6).

$q = P(\kappa)$	κ	$q = P(\kappa)$	κ
0.0000	2975	0.6000	3375
0.0125	3025	0.7000	3425
0.0500	3075	0.7917	3475
0.1125	3125	0.8667	3525
0.2000	3175	0.9250	3575
0.3000	3225	0.9667	3625
0.4000	3275	0.9917	3675
0.5000	3325	1.0000	3725

Given the wavenumber shift $\Delta\kappa$, the shift in wavelength for excitation wavelength λ is [21]

$$\Delta\lambda = \left(\frac{1}{\lambda} - \frac{\Delta\kappa}{10^7} \right)^{-1},$$

where κ is in cm^{-1} and λ is in nm.

Shown in Figure 7 are the probability functions of emitted Raman radiation versus wavelength for incident radiation at four particular wavelengths. Shown are both the results for the approximate PDF of Table 1 and for the function provided in Ref. 21. It can be seen that the emitted Raman radiation is spread over a larger range of wavelengths for high values of incident wavelength than it is for small values of incident wavelength.

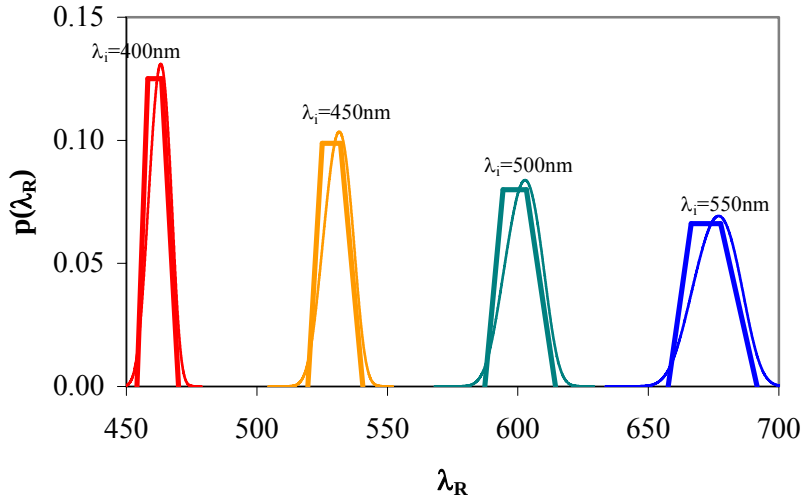

Figure 7 – Raman emission probability functions for 400, 450, 500, and 550 nm. The piecewise-linear profiles are computed from Table 4, and the smooth functions are reproduced from Mobley [21].

5. SOURCES

5.1 Determining The Initial Photon Direction

5.1.1 Source Coordinate System

To determine the initial direction cosines for a photon, we first determine the polar and azimuthal angles θ_s and ϕ_s of the photon relative to the frame of reference of the source (or to the normal to the surface) and then convert θ_s and ϕ_s to μ_x, μ_y, and μ_z. For the special case of a source described in the same frame of reference as the geometry of the problem (e.g., diffuse illumination at a horizontal sea surface), then $\theta = \theta_s$ and $\phi = \phi_s$, and the direction cosines are computed with Eqs. (3.6) - (3.8). If the source frame of reference is not aligned with the axes of the Earth, then one must compute the direction of the source's z-axis with respect to the Earth's frame of reference. If we align the source y-axis along the Earth's x-y plane, then the initial direction cosines of the photon are related to the direction cosines of the source z-axis μ_{xs}, μ_{ys}, and μ_{zs} by [From Eq. (4.14)]

$$\begin{bmatrix} \mu_x \\ \mu_y \\ \mu_z \end{bmatrix} = \begin{bmatrix} \mu_{xs}\mu_{zs}\Big/\sqrt{1-\mu_{zs}^2} & -\mu_{ys}\Big/\sqrt{1-\mu_{zs}^2} & \mu_{xs} \\ \mu_{ys}\mu_{zs}\Big/\sqrt{1-\mu_{zs}^2} & \mu_{xs}\Big/\sqrt{1-\mu_{zs}^2} & \mu_{ys} \\ -\sqrt{1-\mu_{zs}^2} & 0 & \mu_{zs} \end{bmatrix} \begin{bmatrix} \sin\Theta\cos\Phi \\ \sin\Theta\sin\Phi \\ \cos\Theta \end{bmatrix}, \qquad \mu_{zs}{}^2 < 1,$$

$$\begin{bmatrix} \mu_x \\ \mu_y \\ \mu_z \end{bmatrix} = sign\left(\mu_{zs}\right) \begin{bmatrix} \sin\Theta\cos\Phi \\ \sin\Theta\cos\Phi \\ \cos\Theta \end{bmatrix}, \qquad \mu_{zs}^2 \approx 1,$$

where Θ and Φ define the direction of the photon with respect to the *z*-axis of the source.

Let $I(\Theta,\Phi)$ represent the source function, normalized such that

$$\int_0^{2\pi}\int_0^{\pi/2} I(\Theta,\Phi)\ \sin\Theta d\Theta d\Phi = 1\,.$$

For azimuthally independent sources,

$$2\pi\int_0^{\pi/2} I(\Theta,\Phi)\ \sin\Theta d\Theta = 2\pi\int_0^1 I(\mu_s)d\mu = 1\,. \tag{5.1}$$

For azimuthally independent sources (or for modeling azimuthally independent or azimuthally integrated quantities) the probability distribution function for the azimuthal angle is [analogous to Eq. (4.3)],

$$\Phi = 2\pi q. \tag{5.2}$$

The probability density function for the polar angle is therefore

$$p(\Theta) = 2\pi\ I(\Theta)\ \sin\Theta\,,\quad 0\le\Theta\le\pi/2\,,$$

or

$$p(\mu_s) = 2\pi\ I(\mu_s)\,,\quad 0\le\mu_s\le 1\,,\text{ where }\ \mu_s = \cos\Theta\,. \tag{5.3}$$

To determine the initial photon direction in Monte Carlo simulations we set the cumulative distribution function equal to a random number *q*,

$$P(\Theta) = 2\pi\int_0^{\theta_0} I(\Theta)\ \sin\Theta d\Theta = q\,,\quad 0\le\Theta\le\pi/2\,,$$

$$P(\mu_s) = 2\pi\int_{\mu_0}^1 I(\mu_s)\ d\mu_s = q\,,\quad 0\le\mu_s\le 1\,, \tag{5.4}$$

and solve for Θ or μ_s.

For internal sources, let $I(\theta,\phi)$ represent the internal source function normalized such that

$$\int_0^{2\pi}\int_0^{\pi} I(\theta,\phi)\ \sin\theta\ d\theta d\phi = \int_0^{2\pi}\int_{-1}^1 I(\theta,\phi)\ d\mu d\phi = 1\,.$$

As with surface sources, the azimuthal angle is determined with

$$\phi = 2\pi q\,.$$

For azimuthally independent problems,

$$2\pi\int_0^{\pi} I(\theta,\phi)\ \sin\theta\ d\theta = 2\pi\int_{-1}^1 I(\mu)\ d\mu = 1\,, \tag{5.5}$$

which allows us to define the probability density function as

$$p(\theta) = 2\pi\ I(\theta)\ \sin\theta,$$

$$p(\mu) = 2\pi\ I(\mu)\ .$$

To determine the initial photon direction in Monte Carlo simulations we set the cumulative distribution function equal to a random number q,

$$P(\theta) = 2\pi\int_0^{\theta_0} I(\theta)\ \sin\theta\ d\theta = q\ ,\quad 0 \le \theta \le \pi/2$$

$$P(\mu) = 2\pi\int_{\mu_0}^{1} I(\mu)\ d\mu = q\ ,\quad -1 \le \mu \le 1$$

and solve for θ or μ_s.

5.1.2 Ideal Collimated Light

For ideal collimated light (e.g., a laser beam or direct sunlight) we can simply initiate all photons at the same location and pointed in the same direction, all with a weight of unity. For an actual source, however, some amount of variability should be included in the source location and direction.

5.1.3 Isotropic Point Source

For an isotropic point source I is constant. To satisfy Eq. (5.5),

$$I(\theta_s) = I(\mu_s) = \frac{1}{4\pi},$$

so [22]

$$p(\theta_s) = \frac{1}{2}\sin\theta_s, \qquad p(\mu_s) = \frac{1}{2}.$$

The cumulative distribution function is

$$P(\theta_s) = \frac{1}{2}\int_0^{\theta_s} \sin\theta d\theta, \qquad P(\mu_s) = \frac{1}{2}\int_{\mu_s}^{1} d\mu.$$

So, analogous to the result for isotropic scattering,

$$\cos\theta_s = \mu_s = 1 - 2q.$$

5.4.3 Diffuse Illumination

For diffuse illumination, the radiance is constant at all angles. To satisfy Eq. (5.1),

$$p(\mu_s) = \frac{1}{\pi}\mu_s .$$

From Eq. (5.4),

$$P(\mu_s) = 2\int_{\mu_s}^{1} \mu d\mu = 1 - \mu_s^2 = q .$$

Thus,

$$\mu_s = \sqrt{1-q} ,$$

or simply

$$\mu_s = \sqrt{q} .$$

5.2 Initial Photon Position

5.2.1 Ideal Sources

For ideal sources, one simply initiates each photon at the center of the source location.

5.2.2 Gaussian Laser Beam

For a Gaussian laser beam for which b is the $1/e$ radius, the profile of relative irradiance $E(r)$ [mm^{-2}] as a function of radial position r is

$$E(r) = \frac{\exp\left(-r^2/b^2\right)}{\pi b^2} .$$

The probability density function describing the beam profile as a function of radial position r is [23]

$$p(r) = \frac{\exp\left(-r^2/b^2\right)}{b^2} 2r, \quad \text{where} \int_0^\infty p(r)\,dr = 1 .$$

The cumulative distribution function $P(r)$ is

$$P(r) = \int_0^r p(r')\,dr' = 1 - \exp\left(-\frac{r^2}{b^2}\right).$$

Setting $P(r)$ equal to a random number q and solving for r yields

$$r = b\sqrt{-\ln(1-q)} ,$$

which is then the rule for sampling $p(r)$.

5.2.3 Sources for One-Dimensional Problems

Many ocean-atmosphere problems can be reduced to one-dimension, as the desired results frequently depend only on ocean depth. In this case, the 3-dimensional source must be collapsed down to one horizontal location and expressed in terms of intensity per square meter.

5.5 Biased Sampling Of The Source Function

5.5.1 Upward biasing of source polar angle

Suppose we have an isotropic point source and a detector located directly above the source [21]. As shown above, for an isotropic source $p(\theta) = \sin\theta/2$. Because we would like to trace more photons in the upward direction than in the downward direction, we can instead, for example, use

$$p_b(\theta) = \frac{\sqrt{1-\varepsilon^2}}{\pi(1+\varepsilon\cos\theta)}$$

and assign initial photon weights of

$$w = \frac{\pi(1+\varepsilon\cos\theta)}{\sqrt{1-\varepsilon^2}}\frac{\sin\theta}{2}.$$

5.5.2 Biasing the source azimuthal angle

Biasing of the azimuthal angle must be treated differently than polar angle biasing. The azimuthal angle is defined over [0,2π], whereas the polar angle is defined over [0,π]. Also, the probability distribution function for the polar angle contains a sine term arising from spherical geometry, whereas that of the azimuthal angle does not.

If the source is azimuthally symmetric, then the proper probability distribution function is

$$p(\phi) = \frac{1}{2\pi}, \quad 0 \le \phi \le 2\pi .$$

Suppose we wish to bias the photons toward $\phi = 0$, which is along the x-axis. One function that accomplishes this over [0,2π] is

$$p_b(\phi) = \frac{\sqrt{1-\varepsilon^2}}{2\pi(1-\varepsilon\cos\phi)}, \quad 0 \le \phi \le 2\pi .$$

However, because inverse trigonemetric functions return values on [0,π], it is more convenient to work with

$$p_b(\phi) = \frac{\sqrt{1-\varepsilon^2}}{\pi(1-\varepsilon\cos\phi)}, \quad 0 \le \phi \le \pi ,$$

and make adjustments at the end. The proper probability distribution function over $0 \geq \phi \geq \pi$ is $(1/\pi)$, so we assign the photons the initial weight

$$w(\phi) = \frac{(1 - \varepsilon \cos\theta)}{\sqrt{1 - \varepsilon^2}}.$$

The corresponding cumulative distribution function is

$$P(\phi) = 2\left[\frac{\sqrt{1-\varepsilon^2}\,\arctan\left(\dfrac{(1+\varepsilon)\tan(\phi/2)}{\sqrt{(1-\varepsilon)(1+\varepsilon)}}\right)}{\pi\sqrt{(1-\varepsilon)(1+\varepsilon)}}\right].$$

The resulting relationship between ϕ and q is

$$\phi(q) = 2\arctan\left(\frac{\tan\left(\dfrac{q\pi\sqrt{(1-\varepsilon)(1+\varepsilon)}}{2\sqrt{1-\varepsilon^2}}\right)\sqrt{(1-\varepsilon)(1+\varepsilon)}}{1+\varepsilon}\right).$$

If the problem itself (i.e., not just the source) is symmetrical about the $\phi = 0$ direction (i.e., the *x*-axis), we can stop here and let the photons all be initiated on $0 \geq \phi \geq \pi$. Otherwise, generate an additional random number and let

$$\phi = \phi, \quad (q - 1/2) \geq 0,$$

$$\phi = 2\pi - \phi, \quad (q - 1/2) < 0.$$

6. DETECTORS

6.1 Detectors for 3-dimensional problems

Generally we want to measure either the light that is absorbed by the water or the light field that remains. The former is easier to implement in Monte Carlo codes; each time a photon is absorbed we note its location and increment the counter for that location by the absorbed photon's weight. To measure the light field, on the other hand, we need to use logical statements to determine if each photon path crosses the area of the sensor in an appropriate direction.

In three-dimensional problems we generally treat Monte Carlo photons as power [W]. The downward and upward irradiance measurements are computed with

$$E_d(z) \propto \frac{1}{AN}\sum_i w_i, \quad (\mu_z)_i \geq 0\,,$$

$$E_u(z) \propto \frac{1}{AN}\sum_i w_i, \quad (\mu_z)_i < 0\,,$$

where A is the area of the detector and N is the number of photons traced. For radiance detectors we collect the photon weights that reach the detector within the appropriate solid angle and divide the result by the sensor area and solid angle Ω. By definition, $d\Omega = \sin\theta\ d\theta\, d\phi$. For a sensor with a conical field of view (FOV) with half-angle θ_f, the solid angle of its FOV is

$$\Omega = 2\pi\int_0^{\theta_f} \sin\theta d\theta = 2\pi(1-\cos\theta_f)\,.$$

For example, the upwelling radiance is

$$L_u(z) = \frac{1}{2\pi(1-\mu_f)}\frac{\sum w_i}{NA}, \quad (\mu_z)_i \geq \mu_f\,,$$

where μ_f is the cosine of the half-angle FOV ($\mu_f = \cos\theta_f$). The radiance and irradiance at non-vertical orientations are computed in the same manner except that the logical check for admitting photons changes to a comparison between μ_z and the FOV about the normal to the detector.

6.2 Detectors for One-Dimensional Problems

The ocean is frequently approximated as an infinitely wide, plane-parallel medium in which the only variation is with depth. In this case we perform Monte Carlo simulations purely along the z-axis. The Monte Carlo photons in this one-dimensional arrangement represent energy per area [W/m^2] rather than energy [W], and we can take the irradiance [W/m^2] at a given depth to be proportional to the weighted number of Monte Carlo photons that cross the xy plane at that depth. Taking positive z to be the vertically downward direction into the ocean, the downward and upward irradiances normalized to the input flux at the surface are given by

$$E_d(z) = \frac{1}{N}\sum_i w_i, \quad (\mu_z)_i \geq 0,$$

$$E_u(z) = \frac{1}{N}\sum_i w_i, \quad (\mu_z)_i < 0,$$

where N is the number of photons traced and w_i and $(\mu_z)_i$ are the weights and z-direction cosines of the photons that cross depth z. Measurement of the irradiance at directions not perpendicular to the z-axis require that the sum of the photon weights be divided by the z-direction cosine of the normal to the detector to account for the change in photon concentration (photons per area perpendicular to the direction of travel),

$$E(\theta) = \frac{1}{N\cos\theta}\sum_i w_i.$$

For an ideal scalar (spherical) irradiance detector, the detector surface is always perpendicular to the travel direction of photons striking it, and therefore each photon weight should be divided by its own direction cosine $(\mu_z)_i$. For example, the downward scalar irradiance for the one-dimensional geometry is computed with

$$E_{0d}(z) = \frac{1}{N}\sum_i \frac{w_i}{\mu_i}, \quad (\mu_z)_i \geq 0.$$

Radiance measurements (W/m^2/sr) are made by counting only photons that fall within the specified field of view (FOV) and dividing the final result by the corresponding solid angle. For the upwelling radiance the sensor is aligned with the z axis and

$$L_u(z) = \frac{1}{2\pi(1-\mu_f)}\left[\frac{1}{N}\sum_i \frac{w_i}{\mu_i}\right], \quad \mu_i \geq \mu_f,$$

where μ_f is the cosine of the FOV half-angle. More generally, radiance at a nominal viewing angle θ is given by [4]

$$L(\theta) = \frac{E_d(\theta)}{2\pi\ \sin\theta\ \cos\theta\ \Delta\theta},$$

where $E_d(\theta)$ is the irradiance reaching the plane of the sensor within the sensor FOV.

7 SURFACE INTERACTIONS

7.1 Air-Water Interface

7.1.1 On the Air Side

When photons strike an air-water interface, a fraction of them will be reflected and the rest will be transmitted. We therefore need to compute the fraction that is reflected and the directions of the reflected and transmitted packets. The angle of incidence with respect to the normal to the surface $\hat{n}$ is

$$\theta_i = \cos^{-1} | \mu_z \cdot \hat{n} | .$$

The reflected angle θ_r (with respect to the normal to the surface) is the same as the incident angle,

$$\theta_r = \theta_i ,$$

and the transmitted angle θ_t is [21]

$$\theta_t = \sin^{-1}\left(\frac{n_t}{n_i} \sin\theta_i \right),$$

where n_i and n_t are the indices of refraction for the incident side (water) and for the transmitted side (air) of the interface.

For the special case of a horizontal surface,

$$\theta_i = \cos^{-1} \mu_z ,$$

$$\theta_t = \sin^{-1}\left(\frac{n_t}{n_i} \sqrt{1-\mu_z^2} \right).$$

The fractional reflectance for unpolarized light is given by [21, 22]

$$\rho(\theta_i,\theta_t) = \frac{1}{2}\left\{ \left[\frac{\sin(\theta_i-\theta_t)}{\sin(\theta_i+\theta_t)} \right]^2 + \left[\frac{\tan(\theta_i-\theta_t)}{\tan(\theta_i+\theta_t)} \right]^2 \right\}, \theta_i \neq 0,$$

$$\rho(\theta_i) = \left(\frac{n_1-n_2}{n_1+n_2} \right)^2, \quad \theta_i = 0.$$

If we wish to model polarization effects, we can use

$$\rho_\perp(\theta_i,\theta_t) = \left(\frac{n_i\cos\theta_i - n_t\cos\theta_t}{n_i\cos\theta_i + n_t\cos\theta_t} \right)^2 , \tag{7.1}$$

$$\rho_{\|}\left(\theta_i,\theta_t\right)=\left(\frac{n_t\cos\theta_i-n_i\cos\theta_t}{n_t\cos\theta_i+n_i\cos\theta_t}\right)^2, \tag{7.2}$$

$$\rho\left(\theta_i,\theta_t\right)=\frac{\rho_{\perp}+\rho_{\|}}{2}. \tag{7.3}$$

To trace both photons that are reflected and those that are transmitted, we must determine each time a photon reaches the surface whether it is reflected or transmitted. We can do this simply by drawing a random number q and letting the photon reflect if and only if $q \le \rho(\theta_i,\theta_t)$ and transmit if and only if $q > \rho(\theta_i, \theta_t)$. If, on the other hand, we are not interested in the photons that are reflected off the water, we can treat all photons as if they are transmitted and multiply the photon weight by $[1 - \rho(\theta_i,\theta_t)]$. In either case, the total optical pathlength traveled by the photon from one scattering point to the next should equal the value of l computed with Eq. (3.3).

7.1.2 On the Water Side

The angle of incidence with respect to the normal to the surface $\hat{n}$ is

$$\theta_i=\cos^{-1}|\mu_z\cdot\hat{n}|.$$

The reflected angle θ_r (with respect to the normal to the surface) is the same as the incident angle,

$$\theta_r=\theta_i,$$

and the transmitted angle θ_t is [21]

$$\theta_t=\sin^{-1}\left(\frac{n_t}{n_i}\sin\theta_i\right),$$

where n_i and n_t are the indices of refraction for the incident side (water) and for the transmitted side (air) of the interface. For the special case of a horizontal seasurface,

$$\theta_i=\cos^{-1}\mu_z,$$

$$\theta_t=\sin^{-1}\left(\frac{n_t}{n_i}\sqrt{1-\mu_z^2}\right).$$

Because $n_i > n_t$ (i.e., traveling from water to air), there is a critical incident angle θ_c above which there is 100% reflection,

$$\theta_c=\sin^{-1}\left(\frac{n_t}{n_i}\right).$$

The fraction reflected for unpolarized light is given by [21]

$$\rho(\theta_i,\theta_t)=\frac{1}{2}\left\{\left[\frac{\sin(\theta_i-\theta_t)}{\sin(\theta_i+\theta_t)}\right]^2+\left[\frac{\tan(\theta_i-\theta_t)}{\tan(\theta_i+\theta_t)}\right]^2\right\},\quad \theta_i<\theta_c,\theta_i\neq 0,$$

$$\rho(n_1,n_2)=\left(\frac{n_1-n_2}{n_1+n_2}\right)^2,\quad \theta_i=0$$

$$\rho(\theta_i,\theta_t)=1,\quad \theta_i\geq\theta_c.$$

Reflectance for polarized light is provided in Eqs. (7.1) - (7.3). If the surface is horizontal, we can check if the photon is beyond the critical angle by comparing μ_z to μ_c=cos(θ_c),

$$\mu_c=\sqrt{1-\left(\frac{n_t}{n_i}\right)^2}.$$

If we wish to trace both photons that are reflected and those that are transmitted, then we must determine each time a photon reaches the surface whether or not it is internally reflected. If it arrives at an angle greater than the critical angle then it reflects. If not, we can simply draw a random number q and let the photon internally reflect if and only if $q \leq \rho(\theta_i,\theta_t)$. If, on the other hand, we are not interested in the photons that are transmitted, we can treat all photons as if they are internally reflected and multiply the photon weight by $\rho(\theta_i,\theta_t)$. In either case, the total optical pathlength traveled by the photon from one scattering point to the next should equal the value of l computed with Eq. (3.3).

7.1.3 Wind-Blown Surfaces

Let θ_n and ϕ_n represent the polar and azimuthal angles of the normal to a wave facet with respect to the normal to the horizontal surface (i.e., θ_n gives the wave slope, where $\theta_n = 0$ is a horizontal surface, and ϕ_n gives the wave orientation).

The cumulative distribution function for θ_n is [20]

$$P(\theta_n)=1-\exp\left[-\frac{1}{2\sigma^2}\tan^2\theta\right], \tag{7.4}$$

$$\sigma^2=0.003+0.00512U.$$

From (7.4) and (2.3),

$$\tan\theta_n=\sigma\sqrt{-2\ln(1-q)},$$

or, since q is evenly distributed on the interval [0,1], we can write

$$\tan\theta_n=\sigma\sqrt{-2\ln(q)}.$$

The value of ϕ_n is drawn from a different random number [20,11],

$$\phi_n = 2\pi q.$$

The slopes of the wave facet along the *x* and *y* directions are

$$z_x = \frac{dz}{dx} = \tan\theta_n \cos\phi_n$$

and

$$z_y = \frac{dz}{dy} = \tan\theta_n \sin\phi_n.$$

Since the unit vector normal to the wave facet can be written as

$$\hat{n} = \frac{\left[z_x, z_y, 1\right]}{\sqrt{z_x{}^2 + z_y{}^2 + 1}},$$

the angle of the incident photon relative to the face of the wave facet is

$$\cos\theta_i = \left[\mu_x, \mu_y, \left|\mu_z\right|\right] \cdot \hat{n}.$$

Proper implementation of these equations requires some additional logic. At the very least, one must verify that the photon is not impinging on the wave facet from the wrong side [20]. Accommodations should also be made for the possibility of a photon interacting with more than one wave in the same surface interaction and for the fact that not all wave slopes are possible for a given photon incident direction [11, 21].

7.2 Seafloor

7.2.1 General Equations

The interaction of light with the seafloor is quantified by the bi-directional reflectance function that is a function of both incident and reflected directions. Conceptually, we like to think about a light beam traveling in a particular direction (θ_i, ϕ_i) being reflected into another particular direction (θ_r, ϕ_r). But since any source has some finite divergence, and any detector has some finite field of view, we can associate small solid angles $d\Omega_i$ and $d\Omega_r$ with the incident and reflected beams, respectively. Let $L_i(\theta_i, \phi_i)$, and $L_r(\theta_r, \phi_r)$ denote the radiance of the incident beam and the reflected radiance (Figure 8).

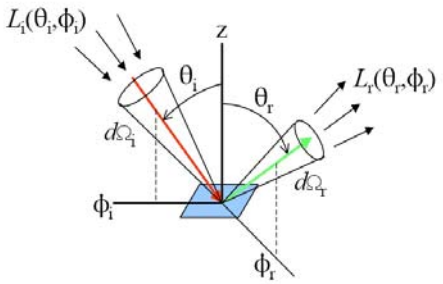

Figure 8 – Quantities used in the definition of the BRDF.

Our goal is to define a quantity that tells us how the reflective properties of the surface vary with incident and reflected directions. Therefore, consider a measurement in which we hold the direction of the detector in Figure 8 constant while we vary the direction of the source. The BRDF is then defined as

$$BRDF\left(\theta_i,\phi_i,\theta_r,\phi_r\right)=\frac{dL_r\left(\theta_r,\phi_r\right)}{L_i\left(\theta_i,\phi_i\right)\cos\theta_i\; d\Omega_i\left(\theta_i,\phi_i\right)} \qquad [\mathrm{sr}^{-1}]. \tag{7.5}$$

Note that if we change only the magnitude of the incident radiance, the reflected radiance will change proportionately, and the BRDF will remain unchanged. However, if we change the direction of the incident or reflected beams while holding all else constant, the BRDF will change.

Suppose we want to compute the total radiance heading upward in direction (θ_r, ϕ_r) owing to light incident onto the surface from all directions. We then rewrite (7.5) as

$$dL_r\left(\theta_r,\phi_r\right)=BRDF\left(\theta_i,\phi_i,\theta_r,\phi_r\right)L\left(\theta_i,\phi_i\right)\cos\theta_i\; d\Omega_i$$

and then integrate over all incident directions to get the total reflected radiance in direction (θ_r, ϕ_r) [21]:

$$\begin{aligned} L_r\left(\theta_r,\phi_r\right) &= \int_{2\pi_i} L_i\left(\theta_i,\phi_i\right) BRDF\left(\theta_i,\phi_i,\theta_r,\phi_r\right)\cos\theta_i d\Omega_i \\ &\equiv \int_{2\pi_i} L_i\left(\theta_i,\phi_i\right) r\left(\theta_i,\phi_i,\theta_r,\phi_r\right) d\Omega_i. \end{aligned} \tag{7.6}$$

where $r(\theta_i,\phi_i,\theta_r,\phi_r)$ is the radiance reflectance function. Clearly, $r(\theta_i,\phi_i,\theta_r,\phi_r) = \cos\phi_i$ BRDF$(\theta_i,\phi_i,\theta_r,\phi_r)$, and the two functions are equivalent ways of describing a surface. Some definitions of BRDF include a factor of π in the numerator of Eq. (7.5). Note that the BRDF is a reflectance per unit solid angle; it can have any non-negative value. As we will see below, only when the BRDF is integrated over solid angle to get, for example, an irradiance reflectance that the result is bounded by one.

It is emphasized that the BRDF completely describes the net effect of everything that happens on or below the surface where it is measured. For example, if the BRDF is measured in the water column 1 meter above a sea grass bed, then all the effects of the light interacting with the grass, sediments, and water below the 1 meter surface are accounted for in this BRDF. Knowing the BRDF on this imaginary surface would, for example, allow Hydrolight (Sequoia Scientific) to compute the radiance distribution in

the region above the depth where the BRDF was measured. Predicting or computing the BRDF of the grass and sediments is quite another story: to do that one must understand all of the extremely complicated interactions of light with the grass and sediment particles.

In a Monte Carlo simulation, we track many individual photon packets as they interact with the medium and its boundary surfaces. In this case, the BRDF must be used as a probability distribution function to determine the direction and weight of the reflected photon packet whenever a photon packet hits the bottom. Given a photon packet with weight w_i that is incident onto the bottom in direction (θ_i, ϕ_i) we need to compute the weight w_r and direction (θ_r, ϕ_r) of the reflected photon packet.

Since the input direction (θ_i,ϕ_i) is known, the BRDF(θ_i,ϕ_i,θ_r,ϕ_r) can be viewed as an (unnormalized) bivariate PDF for the reflected angles θ_r and ϕ_r. Note that, in general, these angles are correlated. The directional-hemispherical reflectance ρ^{dh} for the given (θ_i,ϕ_i) can be computed with

$$\begin{aligned} \rho^{dh}\left(\theta_i,\phi_i\right) &= \int_{2\pi_i} BRDF\left(\theta_i,\phi_i,\theta_r,\phi_r\right)\cos\theta_r \, d\Omega\left(\theta_r,\phi_r\right) \\ &= \int_0^{2\pi}\int_0^{\pi} BRDF\left(\theta_i,\phi_i,\theta_r,\phi_r\right)\cos\theta_r \sin\theta_r \, d\theta_r \, d\phi_r . \end{aligned} \tag{7.7}$$

The reflected photon weight is reduced by ρ^{dh} (i.e., $w_r = \rho^{\mathrm{dh}}(\theta_i,\phi_i)\, w_i$). To determine the new photon direction, we must compute the cumulative distribution functions for ϕ_r and for θ_r. The CDF for the azimuthal angle is given by

$$CDF_\phi\left(\phi_r\right) = \frac{1}{\rho^{dh}\left(\theta_i,\phi_i\right)}\int_0^{\phi_r}\int_0^{\pi/2} BRDF\left(\theta_i,\phi_i,\theta,\phi\right)\cos\theta\sin\theta\, d\theta\, d\phi . \tag{7.8}$$

Note that the directional-hemispherical reflectance is being used to convert the BRDF into a normalized bivariate PDF for θ_r and ϕ_r. We are then integrating out the θ_r dependence to leave a PDF for ϕ_r, which is then being used to construct the CDF for ϕ_r. Setting the CDF equal to a random number ρ from a uniform [0,1] distribution, we must solve the equation

$$\rho = CDF_\phi\left(\phi_r\right) \tag{7.9}$$

for ϕ_r to obtain the randomly determined azimuthal angle of the reflected photon packet. The CDF for θ_r is given by

$$CDF_\theta\left(\theta_r\right) = \frac{\int_0^{\phi_r} BRDF\left(\theta_i,\phi_i,\theta,\phi_r\right)\cos\theta\sin\theta\, d\theta}{\int_0^{\pi/2} BRDF\left(\theta_i,\phi_i,\theta,\phi_r\right)\cos\theta\sin\theta\, d\theta} \tag{7.10}$$

Note that the angle ϕ_r determined in Eq. (7.9) is used in the BRDF in Eq. (7.10) when evaluating the θ integrals. This is how the correlation between θ_r and ϕ_r is accounted for in the determination of the reflection angles. Finally, we draw another random value ρ and obtain the polar angle of the reflected photon packet by solving the equation

$$\rho = CDF_\theta\left(\theta_r\right) \tag{7.11}$$

for θ_r. For all but the simplest BRDFs, the above equations must be evaluated numerically for each photon packet, which can be an enormous computer cost when millions of photon packets are being traced.

7.2.2 Lambertian Surfaces

In many applications we can ignore the directional dependence of the reflection, which is equivalent to assuming that the surface is a Lambertian surface. A Lambertian surface by definition reflects radiance equally into all directions. There is a subtlety in this statement. For a given incident lighting, the number of photons reflected by each point of a Lambertian surface is proportional to $\cos\theta_r$, which is why Lambertian surfaces are sometimes called "cosine reflectors." However, if we view the surface with a radiance detector having a fixed field of view, the area of surface that we are viewing is proportional to $1/\cos\theta_r$. Thus the number of photons going into the detector is independent of θ_r, and the reflected radiance is independent of direction. Its BRDF is simply equal to the constant R_b/π, where R_b is called the reflectivity of the surface or, in this case, the bottom albedo. The reflectivity varies from zero for a completely absorbing ("black") surface, to unity for a completely reflecting surface. There are no Lambertian surfaces in nature, but matte paper is a good approximation except at grazing angles (θ_i and θ_r near 90 degrees), where the surface begins to look shiny.

For a Lambertian seafloor with albedo R_b, we can either let the photon reflect if and only if $q < R_b$ or reflect all photons and multiply the weight by R_b. In either case, the new photon direction is

$$\mu_z = -\sqrt{q},$$

$$\phi = 2\pi q,$$

$$\mu_x = \sqrt{1-\mu_z^2}\cos\phi,$$

$$\mu_y = \sqrt{1-\mu_z^2}\sin\phi.$$

(Recall that each appearance of q is an independent random number.) The new depth z' for a photon reflected off the bottom is

$$z' = -\left(z - z_b\right),$$

where z is the depth ($z > z_b$) the photon would have reached in the absence of the bottom.

7.2.3 Minnaert BRDF

The Minnaert BRDF is

$$BRDF\left(\theta_i,\phi_i,\theta_r,\phi_r\right)=\frac{\rho}{\pi}\left(\cos\theta_i\,\cos\theta_r\right)^k.$$

Note that for $k = 0$ this reduces to the Lambertian BRDF. This BRDF was created to explain the curious fact that the full moon appears almost uniformly bright from the center to the edge of the lunar disk. If the lunar dust were a Lambertian reflector, the full moon would appear bright at the center and darker at the edge. However, the Minnaert BRDF agrees with observation over only a limited range of angles.

Equations (7.7) to (7.11) can be evaluated analytically for the Minnaert BRDF. Equation (7.7) evaluates to

$$\rho^{dh}=\frac{2\rho}{k+2}\cos^k\theta_i,$$

which reduces to $\rho^{dh}=\rho$ for a Lambertian surface. Equation (7.8) gives just

$$CDF_\phi\left(\phi_r\right)=\frac{\phi_r}{2\pi}.$$

Plugging this into Eq. (7.9) and solving for ϕ_r gives

$$\phi_r=2\pi\rho.$$

Thus the azimuthal angle is uniformly distributed over 2π radians. The CDF for θ_r as given by Eq. (7.10) is

$$P\left(\theta_r\right)=1-\cos^{k+1}\theta_r.$$

Equation (7.11) then gives

$$\theta_r=\cos^{-1}\left(\left(\rho\right)^{-(k+2)}\right)$$

after noting that $1-\rho$ has the same distribution as ρ. For a Lambertian surface, the randomly generated θ_r angles are distributed as $\cos^{-1}(\rho^{1/2})$, which certainly isn't intuitive. However, this distribution is precisely what is necessary to make the number of reflected photons per unit solid angle proportional to $\cos\theta_r$.

8. BACKWARD MONTE CARLO SIMULATIONS

When modeling three-dimensional ocean-atmosphere problems, it is often necessary to use Backward Monte Carlo simulations. The Backward Monte Carlo (BMC) approach is most useful for an extended source (e.g., sky radiance onto the sea surface) and a point (or small) detector, which is what commonly exists in oceanography. Only BMC lets us simulate a point-sized detector. Backward Monte Carlo simulation generally refers to ray tracing of photons in the reverse direction; that is, to trace photons from the detector to the source rather than from the source to the detector. Backward MC is useful because it is wasteful to follow simulated photons in the forward direction when very few that are incident on the sea surface are actually collected by the simulated detector. Backward techniques allow us to only follow photons that are pertinent to the final outcome of the simulation. In addition, in the forward direction it is impossible to know how large an area of the sea surface should receive incident photons because that area depends on the local factors of sky conditions, water IOP's, and the location and orientation of the simulated instrument.

Here we will only discuss backward Monte Carlo simulations in the context of problems consisting of a body of water that is illuminated at the sea surface. To implement a BMC simulation, we initiate photons at the position of the detector. The photon's initial direction is determined by sampling from a cumulative distribution function (CDF) designed to reflect the radiance response of the detector. Photons that reach the air-side of the air-water interface are weighted by the probability that a photon would be incident on the seasurface in the exact opposite direction for the given illumination conditions.

For example, consider an upward-facing irradiance detector that measures E_d. Because an irradiance detector has a cosine response to radiance, i.e.,

$$E_d = \int_0^1 \mu_z \, L(\mu) \, d\mu \, ,$$

the probability density function (PDF) for emitting photons from an irradiance sensor in a BMC simulation is proportional to μ_z and the CDF is proportional to μ_z^2,

$$p(\mu_s) = \frac{1}{\pi} \mu_s \, .$$

$$P(\mu_s) = 2\pi \int_{\mu_s}^0 p(\mu) d\mu = 2 \int_{\mu_s}^0 \mu d\mu = -\mu_s^2 = q \, .$$

We therefore generate initial photon directions for a BMC simulation with

$$\mu_z = -\sqrt{q} \, ,$$

$$\Phi = 2\pi q.$$

Shown in Table 6 are example functions for generating the initial directions for a variety of ideal sensors. As always in this report, $\mu_z = 1$ is taken to be the downward direction.

Table 6 – Generating BMC functions for various detector types.

forward-problem detector type	backward MC source function
E_d	$\mu_z = -\sqrt{q}$
E_u	$\mu_z = \sqrt{q}$
E_{0d}	$\mu_z = -q$
E_{0u}	$\mu_z = q$
E_0	$\mu_z = 1 - 2q$
cosine response sensor	$\mu_s = \sqrt{1 - q\sin^2\theta_f}$

For non-ideal sensors, a CDF can be constructed using laboratory measurements. For example, for the Hyper-TSRB (Satlantic, Inc.), the CDF is given in Figure 9 [3,25].

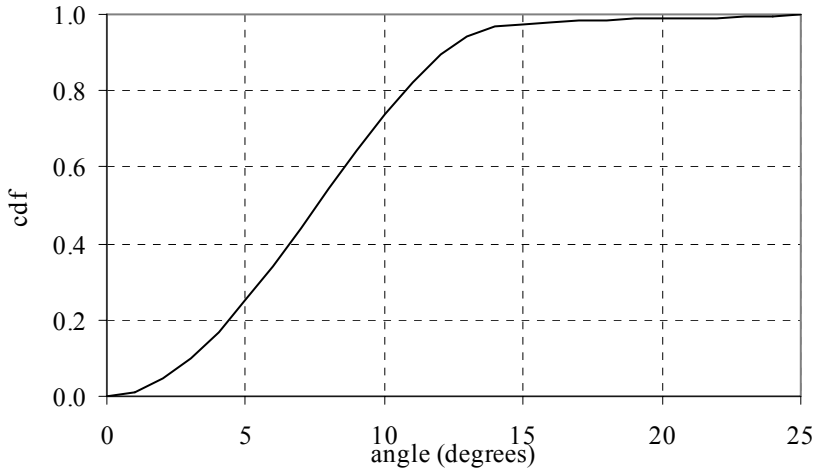

Figure 9 - Cumulative distribution function for the Hyper-TSRB upwelling radiometer (derived from data provided by Satlantic).

See Refs. 7 and 21 for more detailed discussions of the theory behind Backward Monte Carlo calculations.

9. SUMMARY OF FREQUENTLY-USED MONTE CARLO EQUATIONS

Many practical ocean optics Monte Carlo simulations can be formed with the following short list of equations.

The photon geometric pathlength is computed with

$$s = \frac{l}{c} = -\frac{\ln(q)}{c}.$$

Given this pathlength, the photon is moved in the direction of its direction cosines with

$$\begin{bmatrix} x' \\ y' \\ z' \end{bmatrix} = \begin{bmatrix} x \\ y \\ z \end{bmatrix} + \begin{bmatrix} \mu_x \\ \mu_y \\ \mu_z \end{bmatrix} s \, .$$

The azimuthal scattering angle is

$$\Phi = 2\pi q \, .$$

The polar scattering angle depends on the scattering phase function being used. In some cases the angle can be expressed explicitly, e.g.,

$$\mu_s = \cos \Psi_s = 1 - 2q \, , \qquad \text{(isotropic scattering)}$$

$$\mu_s = \frac{1}{2g}\left[1 + g^2 - \left(\frac{1-g^2}{1+g-2gR}\right)^2\right], \quad g \neq 0 \, . \qquad \text{(Henyey-Greenstein scattering)}$$

In other cases, the polar scattering angle must be interpolated from tabulated values. The direction cosines can be updated with

$$\begin{bmatrix} \mu_x' \\ \mu_y' \\ \mu_z' \end{bmatrix} = \begin{bmatrix} \mu_x\mu_z \Big/ \sqrt{1-\mu_z^2} & -\mu_y \Big/ \sqrt{1-\mu_z^2} & \mu_x \\ \mu_y\mu_z \Big/ \sqrt{1-\mu_z^2} & \mu_x \Big/ \sqrt{1-\mu_z^2} & \mu_y \\ -\sqrt{1-\mu_z^2} & 0 & \mu_z \end{bmatrix} \begin{bmatrix} \sqrt{1-\mu_s^2}\cos\Phi \\ \sqrt{1-\mu_s^2}\sin\Phi \\ \mu_s \end{bmatrix}, \quad \mu_z{}^2 < 1 \, ,$$

$$\begin{bmatrix} \mu_x' \\ \mu_y' \\ \mu_z' \end{bmatrix} = sign(\mu_z) \begin{bmatrix} \sqrt{1-\mu_s^2}\cos\Phi \\ \sqrt{1-\mu_s^2}\sin\Phi \\ \mu_s \end{bmatrix}, \quad \mu_z^2 \approx 1.$$

When a photon reaches an air-water interface from the water side, the incident, reflected, and transmitted angles relative to the surface are

$$\theta_i = \cos^{-1} | \mu_z \cdot \hat{n} | \, .$$

$$\theta_r = \theta_i ,$$

$$\theta_t = \sin^{-1}\left(\frac{n_t}{n_i}\sin\theta_i\right),$$

and the fraction of reflected light is given by

$$\rho(\theta_i,\theta_t)=\frac{1}{2}\left\{\left[\frac{\sin(\theta_i-\theta_t)}{\sin(\theta_i+\theta_t)}\right]^2+\left[\frac{\tan(\theta_i-\theta_t)}{\tan(\theta_i+\theta_t)}\right]^2\right\},\theta_i\neq 0,$$

$$\rho(\theta_i)=\left(\frac{n_1-n_2}{n_1+n_2}\right)^2,\quad \theta_i=0.$$

When a photon reaches an air-water interface from the water side, the angles of interest are

$$\theta_i=\cos^{-1}|\mu_z\cdot\hat{n}|.$$

$$\theta_r=\theta_i,$$

$$\theta_t=\sin^{-1}\left(\frac{n_t}{n_i}\sin\theta_i\right).$$

The fraction of reflected light is given by

$$\rho(\theta_i,\theta_t)=\frac{1}{2}\left\{\left[\frac{\sin(\theta_i-\theta_t)}{\sin(\theta_i+\theta_t)}\right]^2+\left[\frac{\tan(\theta_i-\theta_t)}{\tan(\theta_i+\theta_t)}\right]^2\right\},\quad \theta_i<\theta_c,\theta_i\neq 0,$$

$$\rho(n_1,n_2)=\left(\frac{n_1-n_2}{n_1+n_2}\right)^2,\quad \theta_i=0$$

$$\rho(\theta_i,\theta_t)=1,\quad \theta_i\geq\theta_c.$$

where

$$\theta_c=\sin^{-1}\left(\frac{n_t}{n_i}\right).$$

Reflection off a Lambertian surface is handled with

$$\mu_s=-\sqrt{q},\qquad \phi=2\pi q\,.$$

10. EXAMPLE APPLICATIONS

10.1 Collimated Light In A Non-Scattering Medium

Shown in Figure 10 is a simple Matlab script for computing the light intensity at a specified distance from a collimated source in a non-scattering medium. Photons are emitted at position z = 0, and the distance they travel (s) is determined with Eq. (3.4) for the specified attenuation coefficient (c) and the

random number returned by the Matlab function *rand*. Photons that pass the detector position (z_d) are counted. The total measured intensity E is expressed as a fraction of the source intensity. The theoretical result is

$$E = \exp(-c\, z_d),$$

which, for $c = 0.5$ and $z_d = 3$, yields $E = 0.2231$. In a test of the code, running the script in Figure 10 ten times with $N = 10^5$ photons returned a mean value of 0.2230 with a standard deviation of 0.0014.

```
N = 1e5;  % number of photons
zd = 3;     % position of detector
c = 0.5;    % attenuation coefficient
E = 0;      % initialize detector response
for i=1:N
   z = 0;                    % initial photon position
   s = -log(rand)/c;         % geometric path length
   z = z + s;                % move photon
   if z > zd, E=E+1; end     % count photons that reach detector
end
E = E/N            % normalize detector response
```

Figure 10 – Matlab Monte Carlo code for simulating collimated light in a non-scattering medium.

10.2 Irradiances Out The Top Of Scattering Medium

Shown in Figure 11 is a simple Monte Carlo Matlab script for computing the intensities returned from an isotropically scattering semi-infinite medium. The slab is illuminated with collimated light at polar angle $\cos^{-1}(\mu_z)$. The distance each photon travels before its first interaction is determined by Eq. (3.4), at which point the photons's weight is multiplied by the single-scattering albedo ω_0 and the photon is scattered isotropically [Eq. (4.11)]. If and when a photon exits through the top of the scattering medium, then it's weight is added to the count. The count normalized by the number of photons traced gives the intensities leaving the top of the medium. Benchmark numerical results for this problem are provided in Van de Hulst [31, Table 12]. Example results from our Matlab script, along with the corresponding Van de Hulst results, are given in Table 7.

```
    c = 1;       % attenuation coefficient (1/m)
    w0 = 0.8;   % single-scattering albedo
    N = 1e5;    % number of photons to trace
    ns = 100;   % max number of scatters per photon
    E = 0;       % initialize detector
    for i=1:N
       z = 0;         % initial position depth
       muz = 0.1;  % incident light direction (collimated)
       w = 1;         % initial photon weight
       for j=1:ns
          s = - log(rand)/c;              % geometric path length
          z = z + muz*s;                  % move photon
          if (z<0) E=E+w; break, end  % count photons leaving out top
          w=w*w0;                         % absorb fraction of photon packet
          muz= 1 - 2*rand;                % isotopic scattering
       end
    end
E = E/N          % normalize result
```

Figure 11 – Monte Carlo Matlab script for computing the intensities returned from an isotoprically scattering semi-infinite medium.

Table 7 – Comparisons between results from code in Figure 11 with those from Van de Hulst [31].

μ_0	ω_0	Ref. 31 $E_u(0)$	MC $E_u(0)$ mean ; standard deviation (10 runs with N=10^5 each)
1.0	0.8	0.28525	0.2854255 ; 0.000811
1.0	0.4	0.08336	0.0835981 ; 0.000350
0.1	0.8	0.49071	0.4907184 ; 0.001170

10.3 Updating Direction Cosines

Shown in Figure 12 is a Matlab function for updating the direction cosines during a scattering event. This is necessary for simulating anisotropic scattering, such as that in water.

```
function [alp,bet,gam] = chgdir(alpha, beta, gamma, gammas, phis)

% Determines the new direction cosines (alp,bet,gam) from old
%  direction cosines (alpha, beta, gamma), polar scattering cosine
%  (gammas), and scattering azimuthal angle (phis).
%
% Robert A Leathers & Trijntje Downes, 17 March 2000.

stheta = sqrt(1-gamma*gamma);       % sin(theta) of previous photon direction

sthetas = sqrt(1-gammas*gammas);  % sin(theta) of scattering angle
alphas = sthetas*cos(phis);              % x-direction cosine of scattering
betas = sthetas*sin(phis);               % y--direction cosine of scattering

% new photon directions...
if (stheta > 1e-12) % if initial direction not straight up or straight down
   B = [alpha*gamma/stheta, -beta/stheta, alpha;...
        beta*gamma/stheta, alpha/stheta, beta;...
        -stheta, 0, gamma];
   [alphas;betas;gammas];
   newdir = B*[alphas;betas;gammas];
   alp = newdir(1);
   bet = newdir(2);
   gam = newdir(3);
else % initial direction straight up or down (sin(theta)=0)
   % then new direction cosines = +/- scattering direction cosines
   s = sign(gamma);
   alp = s*alphas;
   gam = s*gammas;
  bet = s*betas;
End
```

Figure 12 – Matlab function for updating the direction cosines for anisotropic scattering.

The function in Figure 12 was used to generate Figure 13. An initial photon direction was selected to be $\mu_x = 0.2$, $\mu_y = -0.1$, and $\mu_x = \text{sqrt}(1 - \mu_x^2 - \mu_z^2)$. The scattering polar angle was selected such that $\cos\Psi = 0.4$, and the scattering azimuthal angle was selected randomly using Eq. (4.3). Shown in Figure 13 are the endpoints of 100 unit vectors computed with function chgdir. It can be seen that Eq. (4.3) provides a uniform distribution of the polar scattering angle.

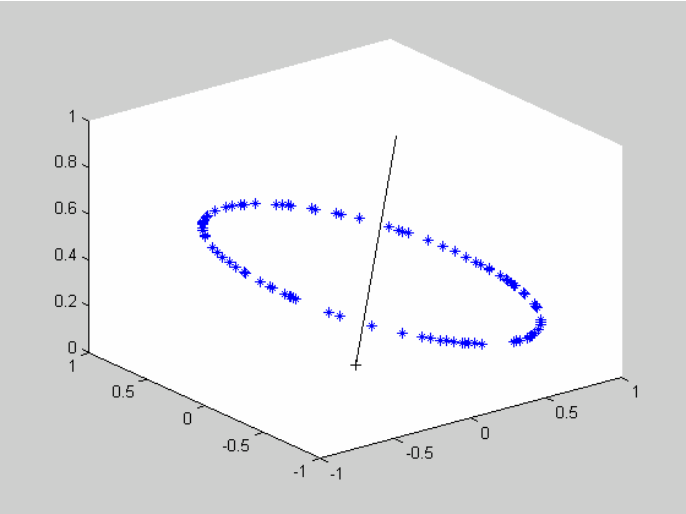

Figure 13 – Example of the random nature of the azimuthal scattering angle.

10.4 3-D Diffusion From Point Source

The code in Figure 14 computes the absorption at a specified radius away from a point source in an isotropically scattering medium.

```
a = 1;   % absorption coefficient (1/m)
c = 6;  % attenuation coefficient (1/m)
w0 = (c-a)/c;  % single-scattering albedo
P0 = 1;     % source intensity (W)
N = 1e4;    % number of photons to trace
ns = 30;   % number of scatters to trace
Nd = 20;    % number of detectors
dd = 0.02; %  detector spacing  (m)
A = zeros(1,Nd);  % initalize detectors (all photons)
for i=1:N
   p=[0,0,0];      % initial position (x,y,z)
   muz = 1-2*rand;  % isotropic source
   phi = 2*pi*rand; % isotropic source
   mux = sqrt(1-muz^2)*cos(phi);  % initial x-direction cosine
   muy = sqrt(1-muz^2)*sin(phi);  % intitial y-direction cosine
   r=0; % intial distance from source
   w = P0;      % initial photon weight
   for j=1:ns
      s = -log(rand)/c;  % geometric path length
      p = p + s*[mux,muy,muz]; % move photon
      r= norm(p);  % radial position
```

```
            index = ceil(r/dd);  % find detector number
            if (index<=Nd), % is photon within detector grid?
               A(index) = A(index) + (1-w0)*w; % count absorption
            end
            w = w*w0;
            mu= 1 - 2*rand;   % isotopic scattering
            phis = 2*pi*rand; % isotopic scattering
            [mux,muy,muz]=chgdir(mux,muy,muz,mu,phis); % new direction
         end
      end
      r = [1:Nd]*dd;  % radii for detectors
      A = A/N;   % normalize detector response
      A1=A1/N;  % normalize detector response
      A = A./(dd*4*pi*r.^2);  % convert response to W/m^3
      ht = 3*a*c*P0*exp(-r*sqrt(3*a*c))./(4*pi*r);   % theory
      semilogy(r,ht,r,A,'*')
      grid on
      xlabel('r'), ylabel('W/m^3')
legend('theory','MC (total)','MC (positive xyz)')
```

Figure 14 – Matlab Monte Carlo code for computing the absorption as a function of radius away from a point source in an isotropically scattering medium.

The theoretical result is given by

$$A = \frac{3acP_0}{4\pi r}\exp(-r\sqrt{3ac}) \tag{10.1}$$

The results from the MC code are compared with the theoretical result in Figure 15.

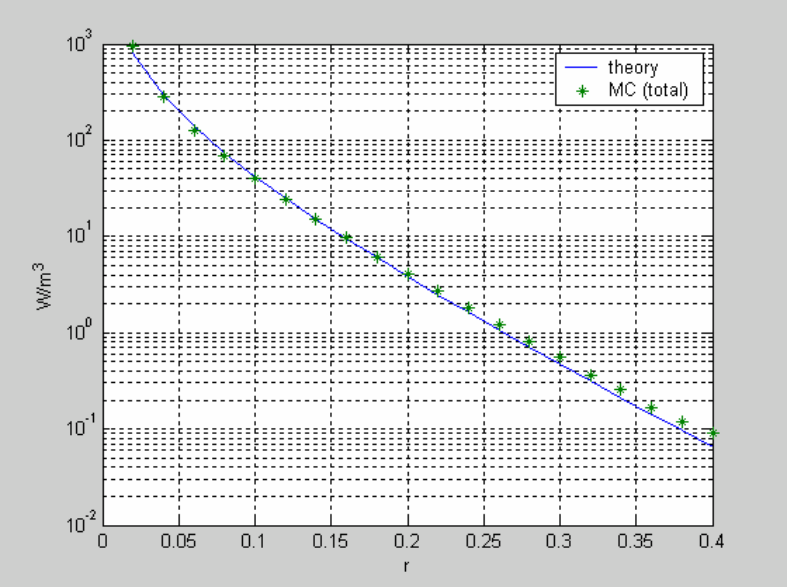

Figure 15 – Comparison of MC result from Figure 14 with theoretical result using 10^4 photons.

10.5 Optically Deep Ocean

Kirk [9] provides example FORTRAN code for a simple 1-dimensional ocean model. Collimated light is incident on a level sea surface. Refraction of the incident light is included but reflection is not. Internal reflection is treated as a step function, where only light below the critical angle is reflected. Water scattering is described by Petzold's measurements in San Diego Harbor. The seafloor is taken to be 100% absorbing and is intended to be located optically far from the surface. No photon weighting is used. Checks are put in place to measure radiance in 5 degree angular bins.

Alternatively, Figure 16 shows our Matlab code for computing upwelling and downwelling irradiances in a homogeneous ocean. Scattering is described by the Henyey-Greestein scattering phase function. Results from the ocean simulation of Figure 16 agreed well with those from Hydrolight (Sequoia Scientific, Redmond, WA).

```
c = 1;      % attenuation coefficient (1/m)
w0 = 0.8;   % single-scattering albedo
g = 0.9;    % scattering asymmetry factor
zd = 1.0;   % depth of downwelling detector
zu = 1.0;   % depth of upwelling detector
n = 1.34;   % relative index of refraction for water
N = 1e4;    % number of photons to trace
ns = 50;   % number of scatters to trace
muc = sqrt(1-1/n^2);  % critical angle for internal reflection
Eu=0; Ed=0; % initiate detectors
for i=1:N
   z = 0;      % initial position depth
   muz = sqrt(rand);  % diffuse illumination
   w = 1;  % initial photon weight
   if (muz==1),
      ra= ((n-1)/(n+1))^2;  % reflection normal to surface
   else
      ti = acos(muz);   % angle of incidence
      tt = asin(sqrt(1-muz^2)/n);  % air-to-water trans. angle
      ra = ((sin(ti-tt)/sin(ti+tt))^2+(tan(ti-tt)/tan(ti+tt))^2)/2;
      muz = cos(tt);  % new direction
   end
   w = w*(1- ra); % air-to-water transmission
   for j=1:ns
      zold=z;  % previous position
      s = -log(rand)/c;  % geometric path length
      z = z + muz*s;     % move photon
      if (z<zu)&(zold>zu), % photon passes Eu sensor
         Eu=Eu+w;   % update upwelling sensor
      end
      if (z<0)          % photon reaches surface
         muz = - muz;   % change to positive value
         z = - z;   % new position of reflected photon
         zold = 0;  % photon now traveling down
         if (muz>muc), % partial transmission
```

```
                if (muz==1),  % photon vertical
                   ra= ((n-1)/(n+1))^2;  % reflection normal to surface
                else
                   ti = acos(muz); % angle of incidence
                   tt = asin(n*sqrt(1-muz^2)); % water-to-air trans. angle
                   rw = ((sin(ti-tt)/sin(ti+tt))^2+(tan(ti-tt)/tan(ti+tt))^2)/2;
                   w = w*rw;  % weight of reflected photon
                end
             end
          end
          if (z>zd)&(zold<zd), % photon passes Ed sensor
             Ed=Ed+w;   % update downwelling sensor
          end
          w=w*w0;   % in-water scattering
          mu = (1+g^2-((1-g^2)/(1+g-2*g*rand))^2)/(2*g); % HG scattering
          Phi = 2*pi*rand;  % azimuthal scattering angle
          muz = muz*mu - sqrt(1-muz^2)*sqrt(1-mu^2)*cos(Phi); % new direction
       end
    end
    disp(sprintf('Eu at %g m: %g',zu,Eu/N));
disp(sprintf('Ed at %g m: %g',zd,Ed/N));
```

Figure 16 – Matlab code for the MC simulation of a homogeneous water column.

10.6 PSICAM Analysis

In the analysis of a Point-Source Integrating-Cavity Absorption Meter (PSICAM) [1], it is useful to know the probability that a photon leaving the inner wall of cavity will return to the wall (as opposed to being absorbed by the water within the cavity). For given water optical properties, this value can be computed with the Matlab code provided in Figure 17. In the absence of scattering, the theoretical result is

$$P_s = \frac{1-\left(2\,a\,r+1\right)\exp\left(-2\,a\,r\right)}{2\,a^2\,r^2},$$

where r is the inner radius of the cavity. The provided code can be used to compute the value for any amount of scattering. It can also be modified to account for non-ideal characteristics of a particular instrument.

```
a = 0.2;      %absorption coeff
b = 50;       %scattering coeff
model = 1;  % 1=isotropic, 2=HG, 3=Petzold
g = 0.92;     %scattering asymmetry factor (required for HG only)
r = 0.05; % radius of sphere (m)
N=1000; %number of photons traced
minweight=0.0001; % min photon weight before discarding it
maxns=10; %maximum number of scatters for each photon

c = a+b; % attenuation coefficient
w0 = b/c; %single-scattering albedo

count=0;
for i=1:N,              % trace photons one at a time
  weight = 1;           % new photon, generated at position (0,0,-r): bottom of sphere
  ns = 0;
  y = 0;
  z = -r;
  x = 0;
  val=(i-0.5)/N; %step uniformly over interval (0,1)
  mu=sqrt(1.0-val);   % diffuse light directions

  gamma = mu; % alpha, beta, gamma = direction cosines
  beta = 0; %move in x-z plane
  alpha = sqrt(1.0-mu^2); %alpha^2+beta^2+gamma^2=1

  while (ns <= maxns) & (weight > minweight)  % keep tracing photon path
    %how far does it go?
    l=-(1/c)*log(1-rand);  %total path length

    z = z+gamma*l;  %new position
    x = x+alpha*l;
    y = y+beta*l;

    if ((x^2+y^2+z^2) > r^2);  %does it reach the wall?
      count=count + weight;
      break %if the photon hits the wall, break out of while loop and don't scatter it.
    end
    % scatter photons
    weight=weight*w0;   % fraction scattered (versus absorbed) given by w0
    ns = ns+1; %number of times the photon has been scattered
    gammas = scat(model,g);  % compute polar scattering angle
    phis = 2*pi*(rand);
    [alpha,beta,gamma] = chgdir(alpha,beta,gamma,gammas,phis);
  end
end
F=count/N;
disp(sprintf('The probability of photon survival from wall to wall is %g',F))
```

Figure 17 – Matlab code for computing the probability of photon survival from wall to wall within a PSICAM.

11. ACKNOWLEDGMENTS

This work was supported by the U.S. Office of Naval Research.

REFERENCES

1. R.A. Leathers, T.V. Downes, and C.O. Davis, Analysis of a point-source integrating-cavity absorption meter, *Appl. Opt.* **39**, 6118–6127, 2000.

2. R.A. Leathers, T.V. Downes, and C.D. Mobley, Self-shading correction for upwelling sea-surface radiance measurements made with buoyed instruments, *Optics Express* **8**, 561–570, 2001.

3. R.A. Leathers, T.V. Downes, C.D. Mobley, and C.O. Davis, *Self-Shading Corrections for Oceanographic Upwelling Radiometers*, U.S. Naval Research Laboratory technical report NRL/FR/7200–04-10,061, 2004.

4. B.M. Concannon and J.P. Davis, Results of a monte carlo investigation of the diffuse attenuation coefficient, *Appl. Opt*. **38**, 5104–5107, 1999.

5. J.P. Doyle and H. Rief, Photon transport in three-dimensional structures treated by random walk techniques: Monte Carlo benchmark of ocean colour simulation, *Math. Comput. Simulat*. **47**, 215–241, 1998.

6. J.P. Doyle and G. Zibordi, Optical propagation within a three-dimensional shadowed atmosphere-ocean field: application to large deployment structures, *Appl Opt*. **42**, 4283–4306, 2002.

7. H.R. Gordon, Ship perturbation of irradiance measurements at sea. 1. Monte-Carlo simulations, *Appl. Opt.* **24**, 4172–4182, 1985.

8. V.I. Haltrin, Theoretical and empirical phase functions for Monte Carlo calculations of light scattering in seawater, in *Fourth international conference on remote sensing for marine and coastal environments*, Proc. ERIM **I509-I518**, 1997.

9. J.T.O. Kirk, Monte Carlo procedure for simulating the penetration of light into natural waters, *Theor. Appl. Genet.* **60**, 197–214, 1981.

10. J.T.O. Kirk, Monte-carlo study of the nature of the underwater light-field in, and the relationships between optical-properties of, turbid yellow waters, *Aust. J. Mar. Fresh Res.* **32**, 517–532, 1981.

11. C.D. Mobley, B. Gentili, H.R. Gordon, Z. Jin, G.W. Kattawar, A. Morel, P. Reinersman, K. Stamnes, and R.H. Stavn, Comparison of numerical models for computing underwater light fields. *Appl. Opt.* **32**, 7484–7504, 1993.

12. A. Morel and B. Gentili, Diffuse reflectance of oceanic waters: its dependence on sun angle as influenced by the molecular scattering contribution. *Appl. Opt.* **30,** 4427–4438, 1991.

13. J. Piskozub, P.J. Flatau, and J.V.R. Zaneveld, Monte carlo study of the scattering error of a quartz reflective absorption tube, *J. Atmos. Ocean. Tech.* **18**, 438–445, 2001.

14. J. Piskozub, A.R. Weeks, J.N. Schwarz, and I.S. Robinson, Self-shading of upwelling irradiance for an instrument with sensors on a sidearm, *Appl. Opt*. **39**, 1872–1878, 2000.

15. G.N. Plass and G.W. Kattawar, Monte Carlo calculations of light scattering from clouds, *Appl. Opt.* **7**, 415ff, 1968.

16. G.N. Plass and G.W. Kattawar, Radiative transfer in an atmosphere-ocean system, *Appl. Opt.* **8**, 415–419, 1969.

17. G.N. Plass and G.W. Kattawar, Monte carlo calculations of radiative transfer in the earth's atmosphere-ocean system: I. flux in the atmosphere and ocean. *J. Phys. Ocean* **2**, 139ff, 1972.

18. L. Roberti, Monte carlo radiative transfer in the microwave and in the visible: biasing techniques, *Appl. Opt.*, 1997.

19. H.H. Tynes, G.W. Kattawar, E.P. Zege, I.L. Katsev, A.S. Prikhach, and L.I. Chaikovskaya, Monte Carlo and multicomponent approximation methods for vector radiative transfer use of effective Mueller matrix calculations. *Appl. Opt.* **40**, 400–412, 2001.

20. K.J. Waters. Monte Carlo modeling of the open ocean light field, Ph.D. thesis, University of California, Santa Barbara, 1994.

21. C.D. Mobley, *Light and Water: Radiative Transfer in Natural Waters*, Academic Press, New York, 1994.

22. H.R. Gordon, Modeling and simulating radiative transfer in the ocean, in R.W. Spinrad, K.L. Carder, and M.J. Perry, editors, *Ocean Optics*, Oxford U. Press, 1994.

23. G.I. Marchuk, G.A. Mikhailov, M.A. Nazaraliev, R.A. Darbinjan, B.A. Kargin, and B.S. Elepov, *The Monte Carlo methods in atmospheric optics*, Springer-Verlag, New York, 1980.

24. L. Wang, S.L. Jacques, and L. Zheng, MCML–Monte Carlo modeling of light transport in multi-layered tissue, *Comput. Meth. Prog. Bio.* **47**, 131–146, 1995.

25. S.A. Prahl, M. Keijzer, S.L. Jacques, and A.J. Welch, A Monte Carlo model of light propagation in tissue, in *Dosimetry of laser radiation in medicine and biology*, Proc. SPIE **IS5**, 1989.

26. L.C. Henyey and J.L. Greenstein, Diffuse radiation in the galaxy, *Astrophys. J.* **93**, 70–83, 1941.

27. T.J. Petzold, Volume scattering functions for selected ocean waters, SIO Ref. 72-78, Scripps Inst. Oceanogr., La Jolla, 79pp., 1972.

28. N.G. Jerlov, *Marine Optics*, Elsevier, New York, 1976.

29. K.J. Waters, Effects of Raman scattering on the water-leaving radiance, J. Geophys. Res. **100**, 13151-13161, 1995.

30. R.A. Desiderio, Application of the Raman scattering coefficient of water to calculations in marine optics, *Applied Optics* **39**, 1893-1894, 2000.

31. H.C. Van de Hulst. *Multiple light scattering*. Academic Press, 1980.